SUPERCONDUCTIVITY AND LOW TEMPERATURE PROPERTIES OF NIOBIUM DISELENIDE SINGLE CRYSTALS GROWN BY DIRECT VAPOR TRANSPORT

by

Norris Earl Lewis

Dissertation submitted to the Graduate Faculty of the
Virginia Polytechnic Institute and State University
in partial fulfillment of the requirements for the degree of
DOCTOR OF PHILOSOPHY
in
MATERIALS ENGINEERING SCIENCE

APPROVED:

Dr. T. E. Leinhardt, Chairman

Dr. D. K. Anderson

Dr. K. L. Reifsnider

Dr. J. G. Dillard

Dr. R. F. Tipsword

Dr. C. R. Houska

Dr. J. P. Wightman

May, 1976

Blacksburg, Virginia

ACKNOWLEDGMENTS

I would like to dedicate this dissertation to my wife, Judy, and my family. The patience and love they have shown and the inspiration and help they have given throughout the past five years has contributed immeasurably to the success of this work.

I wish to express my appreciation for the direction provided by my graduate committee: Dr. T. E. Leinhardt, Chairman; Dr. D. K. Anderson, Dr. J. G. Dillard, Dr. C. R. Houska, Dr. R. F. Tipsword, Dr. K. L. Reifsnider, and Dr. J. P. Wightman. I am especially grateful to Dr. T. E. Leinhardt for the support, direction, and assistance he has provided throughout this work. I wish to express my appreciation to Dr. J. G. Dillard for his assistance and direction with the many XPS measurements that were made. The support given to me by the members of the Physics Department, Drs. S. P. Bowen, J. R. Long, and C. D. Williams, is greatly appreciated. Appreciation is extended to Ms. Debbie Johnson, also of the Physics Department, who typed this manuscript.

The success of this work is in part attributed to the support facilities in the Physics and Chemistry Departments. The Physics Machine Shop staff, Luther Barnett, Melvin Shaver, Robert Ross, and John Gray and the Physics Electronics Shop staff, Al Wyrick, John Painter, and Grayson Wright, are gratefully acknowledged. I wish to recognize Frans van Damme and Andy Mollick of the Glass Shop for the skillful fabrication of the glass apparatus used in this work.

I would also like to extend appreciation to the Director of Engineering at Poly-Scientific, E. W. Glossbrenner, for the consideration

he has shown during the past five years. I am grateful to Poly-Scientific for the experimental hardware that was provided for this work and to the members of the Poly-Scientific staff for their helpful discussions and assistance.

TABLE OF CONTENTS

LIST OF FIGURES

Figure Page

LIST OF TABLES

I. INTRODUCTION

Considerable attention has been given to the dichalcogenides of niobium and tantalum since the early sixties. These compounds along with other transition metal dichalcogenides have been successfully prepared and subjected to studies designed to determine the effect of their two dimensional crystallographic structure upon their low temperature electrical transport properties. $NbSe_2$ in particular has received considerable attention because it has the highest superconducting transition temperature among the layered-structure transition metal dichalcogenides. Much of the work performed on these compounds throughout the sixties has been summarized by Wilson and Yoffe.[1]

Revolinsky et al.[2] have shown that seven phases exist within the composition limits of NbSe to $NbSe_3$. Of these seven phases more attention has been given to the 2H-$NbSe_2$ and 4H-$NbSe_2$ phases since they are superconducting. The 2H-$NbSe_2$ phase has a two-layered hexagonal structure of the NbS_2 type and the 4H-$NbSe_2$ is a four-layered hexagonal structure of a new type. In these structures the layers consist of two parallel anion sheets between which is a sheet of cations. In both 2H and 4H polytypes the cations are coordinated by a trigonal prism of selenium anions as shown in Figure 1. The bonding between layers is van der Waals type between anions while the bonding within the layers is stronger and is a mixture of covalent and ionic bonds.[3] The layer structure of this compound gives rise to anisotropic transport properties.

The possibility of studying the properties of electrons constrained

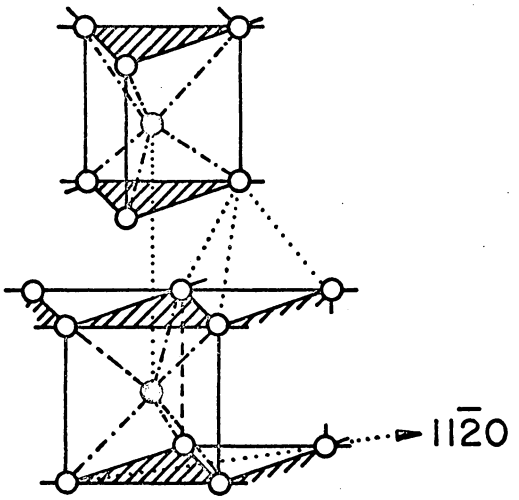

2H-$NbSe_2$

○ NIOBIUM

○ SELENIUM

× DENOTES LOCATION OF INTERSTITIAL ATOMS

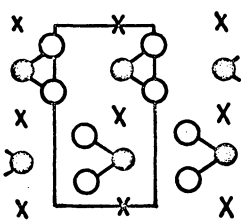

2H-$NbSe_2$
11$\bar{2}$0 SECTION

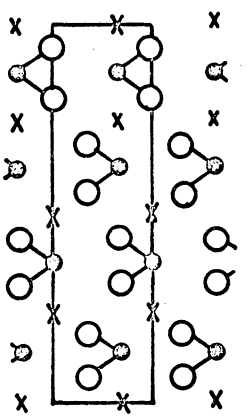

4H-$NbSe_2$
11$\bar{2}$0 SECTION

FIGURE 1. Structure of 2H-$NbSe_2$ and 4H-$NbSe_2$ (After Wilson and Yoffe[1]).

to flow in only two dimensions has been responsible for much of the interest in the layered compounds. In addition to this, the search for new mechanisms of superconductivity which involve interactions between conduction electrons and organic molecules as proposed by Little[4], Ginzburg[5], and others has stimulated additional interest in these compounds. The ability to insert organic molecules between the layers (intercalation) of compounds such as TaS_2, NbS_2, and $NbSe_2$ has provided a means of constraining conduction electrons to thinner layers than those prepared by vacuum deposition as well as placing the organic molecules in close proximity to the metallic layers.[6] Although no evidence has been found for new mechanisms of superconductivity in these intercalation complexes, study is continuing because of the highly anisotropic properties they possess.

In the case of 2H-$NbSe_2$, studies have not been limited to the areas of intercalation. The dependence of superconducting transition temperatures (T_c) on changes in chemical composition and crystal structure has been studied[2,7]. Superconducting transition temperatures were shown to decrease from a temperature of 7°K to about 2°K in a regular manner as the sample composition changed from $NbSe_2$ to $Nb_{1.05}Se_2$. The change to T_c was attributed to a rearrangement of the niobium sublattice. Spiering et al.[8] demonstrated that anomalies in critical current versus magnetic field measurements were related to chemical composition. Antonova et al.[9] studied the effect of crystal disordering, which resulted from changes in composition, upon superconducting critical currents.

The temperature dependence of the electrical resistivity and the

Hall coefficient of single crystals of 2H-$NbSe_2$ was measured by Lee et al.[10]. The Hall coefficient was observed to undergo a change in sign at about 26°K. Above this temperature the crystals were p type and below this temperature they were n type. The Hall coefficient, magnetoresistance, and thermoelectric power were measured as a function of temperature and crystal orientation by Huntley and Frindt[11]. In this study a correlation was observed between the Hall coefficient and the sample residual resistivity ratio (RRR). The Hall coefficient was observed to change sign at about 27°K for pure samples (high RRR) while those containing larger amounts of iodine (low RRR) did not undergo a change of sign. Yamaija et al.[12] studied the pressure dependence of T_c and from this data concluded that the change in sign of the Hall coefficient was caused by a crystallographic structure change.

Marezio et al.[13] used single crystal x-ray diffraction data to show that 2H-$NbSe_2$ undergoes a structural distortion at 40°K. They deduced that the coupling of the niobium atoms is the driving mechanism for the crystallographic distortion. Thompson[3] concluded from a systematic study of the crystal distortions that occur in $NbSe_2$ and other layered compounds that a correlation exists between distortion temperatures and the fractional ionicity of the metal-chalcogen bond. Wilson et al.[14] have used electron diffraction data to propose that charge density waves, Fermi surface instabilities, occur in layered compounds and cause the crystal distortions. It has been experimentally determined that low temperature crystallographic distortions occur in 2H-$NbSe_2$ which appear to explain anomalies that have been observed in electrical properties such as the Hall coefficient and the resistivity.

The mechanism causing these distortions is not completely understood at the present time.

Several experiments have been performed to determine the effect of the anisotropic structure of 2H-$NbSe_2$ on properties such as electrical resistivity and the superconducting energy gap. Edwards and Frindt[15] investigated the temperature dependence of the electrical resistivity parallel and perpendicular to the c-axis. They determined that the ratio of the parallel and perpendicular resistivities was a constant 31:1 over the temperature range of 300 to 80°K. A linear decrease in this ratio with temperature was observed below 80°K. Frindt et al.[16] observed a decrease for the anisotropy in the electrical resistivity with pressure. A value of about five was measured for the ratio of the parallel and perpendicular resistivities at a pressure of 33 kb at 300°K.

The anisotropy of the superconducting energy gap of $NbSe_2$ was determined from far-infrared transmission spectra[17]. The value of the energy gap for electrons flowing parallel to the c-axis was observed to be 1.25 meV while that for electrons flowing perpendicular to the c-axis was observed to be 2.15 meV at 1.6°K. Morris and Coleman[18] measured the energy gap for electrons flowing parallel to the c-axis using electron tunneling methods. The tunnel junctions studied by these investigators were made with carbon barriers rather than metal oxide barriers which are frequently used in tunneling experiments. An energy gap of 1.24 meV was observed at 1.1°K. Lee et al.[19] measured an energy gap of 1.15 meV at 1.5°K for electrons flowing parallel to the c-axis using a niobium point contact tunneling method.

The single crystals of 2H-$NbSe_2$ used in all the areas of research mentioned above were prepared by a chemical transport procedure that was originally described by Schafer[20] and Nitsche et al.[21]. In more recent years the procedure given by Kershaw et al.[22] has been frequently used. The chemical vapor transport method involves vaporization of the polycrystalline compound by forming a volatile chemical intermediate and utilizing the temperature dependence of the chemical equilibrium to reform the compound at a lower temperature. In the case of 2H-$NbSe_2$ single crystals the principal transporting agent has been iodine. The equilibrium that is involved in this case is:

$$NbSe_2 + 2I_2 \rightleftarrows NbI_4 + 2Se \ . \qquad (1)$$

The formation of single crystals proceeds as follows. The chemical intermediate, NbI_4, forms in the vaporization end of a horizontal tube near the polycrystalline $NbSe_2$ charge. A crystallization region of the tube is maintained at a lower temperature. As the NbI_4 and Se move into the crystallization region, $NbSe_2$ reforms and deposits as single crystals. The iodine is set free because of the temperature dependence of NbI_4 and then diffuses back to the vaporization area of the tube to transport more $NbSe_2$.

The work presented here deals with the growth of single crystals of 2H-$NbSe_2$ by a direct vapor transport (DVT) procedure. The significant feature of this procedure is that this material can be prepared in a form free of the halide transporting agent. Initially it was assumed that little, if any, transporting agent remained in the crystal after the growth process.[10,22] Later it was shown that significant

quantities of iodine can be incorporated in the lattice by this procedure.[11,23,24]

It has been the purpose of this work to gain an understanding of the DVT growth mechanism and how the growth parameters affect crystal properties. Single crystals of 2H-$NbSe_2$ prepared by the DVT and iodine vapor transport (IVT) procedures have been studied in a parallel fashion. The principal impact of this work, through the availability of DVT crystals, has been to determine the effect of iodine on the transport properties of 2H-$NbSe_2$. Huntley and Frindt[11] addressed the problem of low temperature electron scattering by iodine and structural defects. However, in their work they did not have crystals free of iodine and, therefore, could not completely differentiate between structural defects induced by other means and those caused by the presence of iodine.

The results being presented have been arranged as follows:

A. Crystal Nucleation and Growth

The effects of deviations from stoichiometery and reaction and annealing times on DVT crystal transport properties are discussed.

B. Crystal Characterization

The results of neutron activation analysis, x-ray photoelectron spectroscopy, and x-ray diffraction studies that were performed on both types of crystals have been presented. The interpretation of the low temperature transport measurements have been made using these results where possible.

C. Low Temperature Transport Measurements

Superconducting transition temperatures (T_c), superconducting

transition temperatures versus current densities (T_c vs J), critical current densities versus thicknesses (J_c vs t), and residual resistance ratios (RRR) were measured for DVT and IVT crystals. The differences observed in the properties of these samples have been explained using the data from the literature and the data collected in this work.

Crystals grown by the DVT procedure were subjected to heat treatment in vacuum and an iodine atmosphere. The effect upon T_c, J vs T_c and RRR was measured. These observations have been interpreted in view of other experiments designed to study the effect of impurities[11] and structural defects[25] on the electrical transport properties of 2H-$NbSe_2$.

Electron tunneling measurements were made on DVT and IVT samples using carbon as a tunneling barrier. The results from these experiments were compared to values from the literature for IVT crystals.

II. EXPERIMENTAL

A. Crystal Nucleation and Growth

All of the DVT and IVT single crystals discussed in this work were prepared from a single lot of niobium (99.9%) and two different lots of selenium (99.999%). These materials were purchased from the Apache Chemicals Company. One batch of single crystals was prepared by the IVT procedure described by Kershaw, et al.[22]. Nine batches of single crystals were prepared by the DVT procedure. These have been identified as DVT 1, DVT 2, ..., DVT 9. Data were taken from single crystals from the IVT batch and seven of the nine DVT batches. The individual single crystals taken from each of these batches have been identified as IVT 1A, IVT 1B, DVT 1A, DVT 1C, etc., to avoid confusion when more than one crystal from the same batch has been characterized.

At the beginning of this effort, more emphasis was placed upon superconductivity and other electrical transport properties than upon nucleation and growth. After a limited number of transport measurements, T_c, T_c vs J, and RRR, were made and it was discovered that the RRR values of the DVT samples were higher than any IVT values published in the literature, more emphasis was placed on growth conditions. The growth parameters that were studied were limited to deviations from stoichiometry, initial reaction times, times at growth temperature, and annealing times.

The DVT method involves placing the desired quantities of Nb and Se in quartz tubes measuring 0.15m in length by 0.02m in O.D. Prior to sealing, the tubes are evacuated to a pressure of less than 5×10^{-3} torr

as measured with a thermocouple gauge. The tubes were then placed in a horizontal multi-zone furnace with the charge spread evenly over the bottom half of the tube and heated uniformly according to the procedures outlined in Table I. Several Chromel-Alumel thermocouples were placed along the length of each tube so that temperature uniformity could be monitored. Temperatures were measured to within ± 15°K. The total charge weight in all cases was approximately 16 grams.

B. Crystal Preparation for Characterization

It was necessary to determine the thickness of each of the crystals in order to calculate the current density. The current density calculated from the current flowing through the sample and the sample cross-sectional area is an apparent current density. It is possible that all layers of the sample may not conduct uniformly and, therefore, the real current density may be much higher than the apparent current density. In those instances where the crystals were thick enough (0.01 cm - 0.005 cm) the thickness was measured using an optical microscope equipped with a filar eyepiece. The thicknesses of some of the thinner crystals were measured with a Unitron metallograph where magnifications greater than 25X were possible. It was necessary in some cases to cut the crystals into rectangular shapes, the dimensions of which could be measured accurately with a filar eyepiece. Thicknesses were then calculated using crystal masses and density. The latter was determined from lattice parameters. Huntley and Frindt[11] used a density of 6.43 g/cc calculated from lattice constants to determine the thickness of their IVT crystals. A third means of determining the thicknesses of the thinner crystals was to use a resistivity value which was calcu-

TABLE I. PROCEDURE USED FOR PREPARING DVT CRYSTALS

Batch Chemical Formula	DVT 1 $NbSe_2$		DVT 2 $NbSe_2$		DVT 3 $NbSe_2$		DVT 4 $Nb_{0.97}Se_2$	
GROWTH SEQUENCE	TEMP(°K)	DAYS	TEMP(°K)	DAYS	TEMP(°K)	DAYS	TEMP(°K)	DAYS
1. Slow heat and hold at indicated temp.for initial reaction	775	7	600 600→825 825	1 6	805	4	820	4
2. Agitation in tube at room temperature	10-15 min.		10-15 min.		10-15 min.		10-15 min.	
3. Reaction time at indicated temperature	850	6	825	6	810	3.5	820	3.5
4. Agitation in tube at room temperature	10-15 min.		10-15 min.		10-15 min.		10-15 min.	
5. Slow heat to indicated temperature	300→850 850 850→1200	1	1200		1200		1200	
6. Time at indicated temperature	1200	7	1200	14	1200	10	1200	10
7. Slow cool to intermediate temperature	1200→1015		1200→1015		1200→1115 1115 1115→1025	 1	1200→1115 1115 1115→1025	 1
8. Time at indicated temperature	1015	4	1015	12	1025	6	1025	6
9. Cool to 300°K		4 hrs		4 hrs		4 hrs		4 hrs

TABLE I (Cont.). PROCEDURE USED FOR PREPARING DVT CRYSTALS

Batch Chemical Formula	DVT 5 $NbSe_2$		DVT 6 $Nb_{0.95}Se_2$		DVT 9 $Nb_{1.05}Se_2$		DVT 9 $Nb_{1.05}Se_2+0.1Se \xrightarrow{\Delta} 1.05NbSe_2$	
GROWTH SEQUENCE	TEMP(°K)	DAYS	TEMP(°K)	DAYS	TEMP(°K)	DAYS	TEMP(°K)	DAYS
1. Slow heat and hold at indicated temp. for initial reaction	790	3	795	3	775	9	795	1
2. Agitation in tube at room temperature	10-15 min.		10-15 min.		10-15 min.		10-15 min.	
3. Reaction time at indicated temperature	790	3	795	3	825	6	825	3
4. Agitation in tube at room temperature	10-15 min.		10-15 min.		10-15 min.		10-15 min.	
5. Slow heat to indicated temperature	1200		1200		1210		1200	
6. Time at indicated temperature	1200	9	1200	9	1210	7	1200	9
7. Slow cool to intermediate temperature	1200→1025		1200→1025		1200→1000		1200→1125 1125 1125→1025	1
8. Time at indicated temperature	1025	4	1025	4	1000	7	1025	2
9. Cool to 300°K		4 hrs		4 hrs		4 hrs		4 hrs

lated for crystals thick enough to measure optically with sufficient accuracy.

It was necessary to cleave the IVT and DVT crystals to gain information about the oxidation state of niobium on the surface and in the interior of the crystals. Since an inverse relationship between critical current density and sample thickness has been observed for 2H-$NbSe_2$[26] and since the IVT crystals grew much thicker than the DVT, it was necessary to cleave the former to approximately the same thickness as the DVT's so that the critical current density data could be compared on an equal footing. The IVT crystals were cleaved perpendicular to the c-axis by inserting a sharp blade parallel to the basal plane and peeling away the layers with tweezers. In some instances these cleaved pieces were used for neutron activation and analyses. The crystals that were too thin to handle in this fashion were cleaved by pulling successive layers away with sticky tape.

C. X-Ray Diffraction Equipment

Powder x-ray diffraction patterns were prepared using a General Electric XRD-5 diffractometer. The diffractometer was equipped with a nickel filtered copper K_α (λ=1.5404 Å) x-ray tube and a standard Geiger Mueller detector. Beam and detector slits were 1° and 0.1° respectively. The output of the detector was fed into a pulse height analyzer and from there to a linear recorder. Single crystals were attached to the diffractometer sample holder using Apiezon L grease. This method of mounting the sample allowed the crystals to be removed for other studies by dissolving the grease with benzene. Powder samples were presented to the diffractometer using tape with adhesive on both sides.

Back scattering and transmission Laue photographs were made of single crystals using a Land XR-7 diffraction cassette attached to the XRD-5 diffractometer. All transmission and back scattering photographs were made with a crystal-to-film distance of 3.0 cm, a 0.01 cm collimator, and Polaroid Type 57 film. The copper x-ray tube was operated at 25 KV and 25 ma for all photographs. Exposure times for transmission photographs were typically 5 to 10 minutes, while the exposure times required for back scattering photographs were 30 to 45 minutes. Single crystals were mounted on the sample holder of the goniometer using Apiezon L grease. In all cases the incident x-ray beam was parallel to the crystal c-axis.

D. X-Ray Photoelectron Spectroscopy Equipment

An AEI ES-100 spectrometer was used to measure the x-ray photoelectron spectra (XPS). The aluminum $K_{\alpha 1,2}$ line (1486.6 eV) was the source of x-ray excitation in all cases. The equation describing the energy of the photoelectrons ejected from the sample can be written as

$$E_K' = h\nu - E_b - \phi_s - \phi \qquad (2)$$

where E_K' is the kinetic energy of the emitted electron, $h\nu$ is the x-ray energy, E_b is the electron binding energy, ϕ_s is the work function of the sample and ϕ is a correction factor for charge build up on the sample. In all cases discussed in this work the sample and spectrometer were electrically common so the ϕ term can be ignored. The kinetic energy E_K of the electron, which is what the spectrometer measures, is related to E_K' by the relation

$$E_K = E_K' + (\phi_s - \phi_{sp}) \tag{3}$$

where ϕ_{sp} is the work function of the electron-analyzer material. Thus the expression for the binding energy of the electron can be written as

$$E_b = h\nu - E_K - \phi_{sp} \ . \tag{4}$$

Usually ϕ_{sp} is empirically determined from materials such as carbon or gold whose binding energies are accurately known. The absolute binding energy for the C $1s_{1/2}$ level of carbon in the sample was measured to be 284.2 eV. The binding energy of the Au $4f_{5/2}$ and 4 $f_{7/2}$ levels were determined relative to C $1s_{1/2}$ level of carbon and these valves were found to be 87.1 eV and 83.4 eV, respectively.[27]

Samples were presented to the spectrometer as single crystals or as polycrystalline powders. The samples were attached directly to a gold-plated rectangular probe which also served as a gold standard. In the experiments where the single crystals were cleaved after the "as grown" surfaces were characterized, the samples were attached to the probe using a cellophane tape with adhesive on both sides. Thus single crystals could be cleaved without being removed from the probe by using a second piece of tape to lightly pull away surface layers. All cleaving operations were performed in air. Single crystals were powdered and dusted on double adhesive tape for the experiments requiring a large amount of crystal surface area. All spectra were measured at room temperature and a pressure of 10^{-8} torr.

A Digital Equipment Corporation PDP-8/e computer and a AEI-DS100 data system were used to control the spectrometer scanning function

such as energy region, number of energy levels scanned, length of scan and output functions. The data were plotted on a Hewlett-Packard Model 2D-2AM X-Y recorder interfaced to a Digital Equipment Corporation PDP-8/I computer using the MADCAP IV* program. Point data were smoothed using an 11-point parabolic least squares smoothing routine and plotted as a line plot.

E. Low Temperature Apparatus

In most instances the crystals grown by the DVT procedure were thinner and more delicate than those grown by the IVT procedure. A multiprobe apparatus which would neither tear nor strain the delicate DVT crystals and also handle the thicker, less compliant IVT crystals was constructed to measure T_c, T_c vs J, RRR, and electron tunneling characteristics of the crystals. This apparatus consisted of seven 0.04 cm diameter electrical contacts spaced 0.125 cm apart on an epoxy base. These contacts were raised approximately 0.02 cm above the epoxy base and formed contacts for seven mating 0.018 cm diameter Paliney 7 cantilevered electrical contacts (Figure 2). The contact pressure exerted on the sample was adjusted by bending the fingers at the point of exit from the insulator block. Once the contact pressure was set it was possible to lift the fingers and insert a sample without exceeding the yield stress of the fingers. This design allowed the crystals to be readily removed or reinserted without damage. The purpose of seven equally spaced electrical contacts for each crystal side was to

* MADCAP = A multiplexed ADC and Analog Plotter Program. Written by G. W. Dulaney, Digital Equipment Corporation, Maynard, Massachusetts.

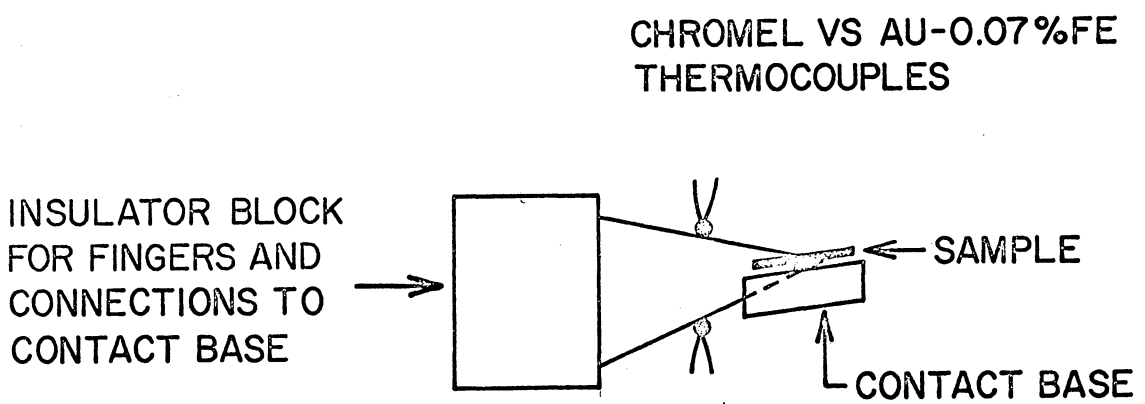

FIGURE 2. Multiprobe Sample Holder for Low Temperature Measurements.

accommodate a range of crystal lengths and to allow four probe measurements either parallel or perpendicular to the crystal c-axis. This contact arrangement also allowed current connections to be made to both faces of the crystal to get a more uniform current density in the crystal when four probe measurements were being made. Finally, the four contact geometry required for measuring current vs voltage characteristics of superconducting tunnel junctions was readily achieved with this apparatus.

When low temperature measurements were made, the multiprobe apparatus was located in a copper container as illustrated in Figure 3. Temperatures above 4.2°K were achieved by passing a current through two series connected ten ohm resistors cemented to the base of the copper container. Thus, when the helium level was below the resistors, temperatures up to 7.5°K readily could be attained. Reference junctions for the Chromel vs Au-0.07 At. % Fe thermocouples were located on copper blocks which were suspended below the helium level. The thermocouples were calibrated by measuring the transition temperature (7.19°K) of thick lead samples vapor deposited on mica substrates. The slope of the thermocouple temperature vs voltage curve at 7°K was measured to be 0.069°K/μv.

Thermocouple voltages as well as sample voltages were measured with an uncertainty of ± 0.2μv using K-3 potentiometers (Figure 4).

F. Neutron Activation Analysis

The neutron activation analyses were performed by the Virginia Polytechnic Institute and State University Neutron Activation Analysis Laboratory. Samples of $NbSe_2$ from several different growths and the

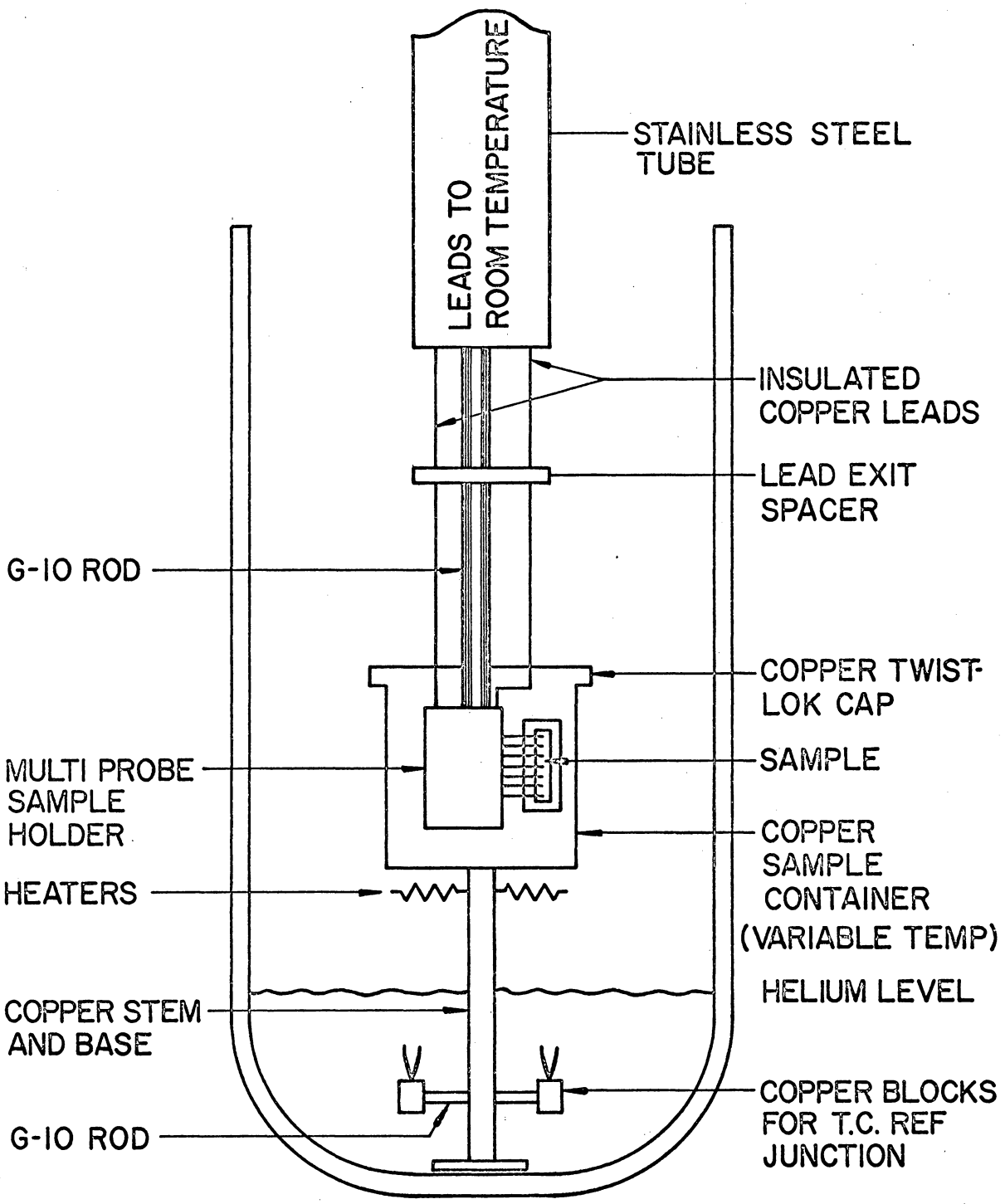

FIGURE 3. Cryostat for Low Temperature Measurements.

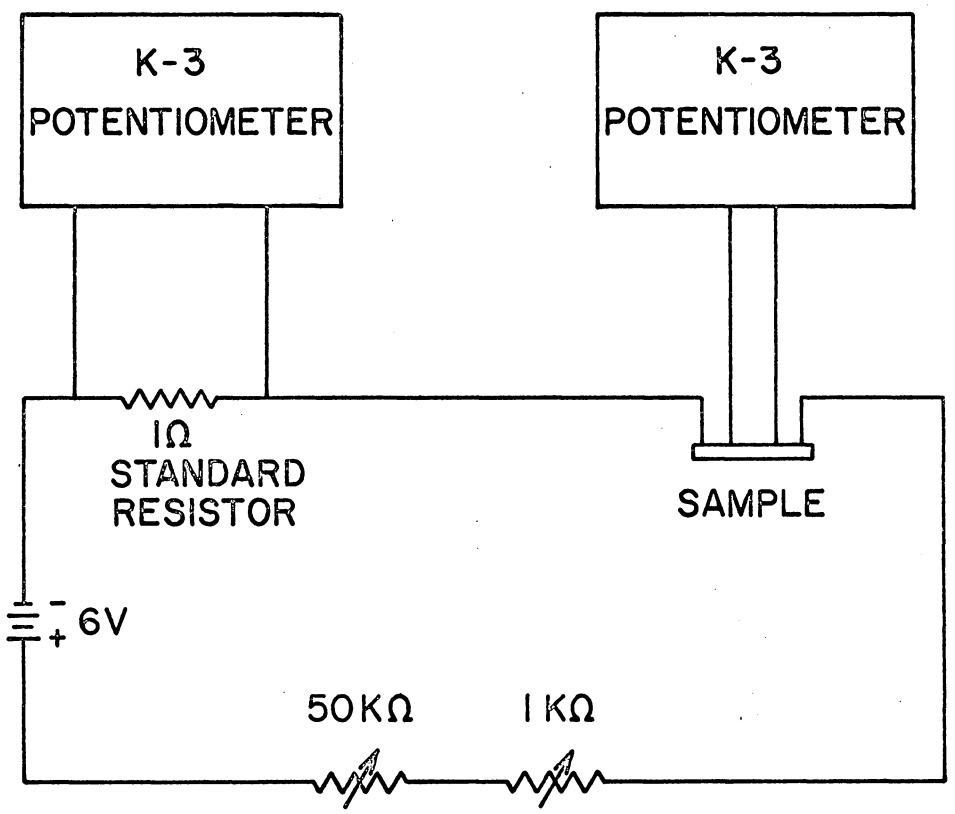

FIGURE 4. Circuit for Measuring Transition Temperature, Transition Temperature Versus Current Density, and Residual Resistivity Ratio.

niobium and selenium used to prepare these samples were analyzed by this method. The samples were irradiated in a thermal flux of 1.3 x 10^{12} n/cm^2 - sec. Neutron activation times of seconds were required to detect iodine while times of seven hours were required for elements such as copper, chromium, cobalt, iron, potassium, sodium, zinc, and several others. The activity of the samples was high after the long activation period and could not be counted for several days. When the analysis for iodine was performed, the samples were counted within seconds of the activation time.

Difficulty was encountered with the analysis of the $NbSe_2$ and selenium samples because of the Se^{75} isotope. This isotope has a half life of 120 days which is the reason a long waiting period was necessary before the samples could be counted. Small sample masses (2-3 mg) were used to minimize the interference of the Se^{75} isotope. However, the smaller sample mass reduced the ability to accurately measure small quantities of elements that do not readily activate such as iron.

The sensitivity for each of the elements detected in the samples used in this study have been listed in Table V on page 60. The error in the measurements is about ± 10 percent of the amount present. In some cases the error in the iron measurements is ± 55 percent of the amount present.

G. Apparatus and Procedure For Iodine Diffusion Studies

The DVT single crystals and polycrystalline material which were to be doped with iodine were placed in a 2.0 cm O.D. quartz tube, fabricated with a sealing constriction and attached to a glass manifold with a ground glass joint. This manifold was connected to a glass and tef-

lon valve which served as an isolation valve from the vacuum line. The iodine was contained in a small bulb having a volume of 2-3 cm^3 which was connected to the manifold with a side arm and a glass and teflon valve. The valves were arranged so that the single crystals and polycrystalline charge could be degassed as long as desired while the bulb containing the iodine was held at atmospheric pressure. After the degassing operation was completed, the bulb containing the iodine was evacuated to a pressure of 10 microns and held there for the desired time. The entire manifold was closed to the vacuum line while the iodine was sublimed into the charge area. This was accomplished by heating the bulb containing the iodine and the connecting tubing while the charge area was held at liquid nitrogen temperature. Sublimation of the iodine from a side arm in this manner rather than placing it in with the charge eliminated the transfer of nonvolatile contaminants in the iodine to the sample. After the iodine transfer was completed, the isolation valve to the vacuum line was opened for 1-2 minutes before the tube was sealed. The tube was removed from the manifold, placed in a horizontal furnace, heated to a temperature of 975°K, and held there for the desired time.

Three samples of DVT 1 powder were used in trial experiments to determine the amount of iodine needed to obtain a concentration of 100-600 ppm in the crystals after diffusion. Each sample of powder weighed approximately 300 mg. The quantity of iodine placed in the bulb was approximately 1 mg. The quantity of iodine transferred to the charge area was determined by the length of time the bulb was evacuated prior to the transfer step. After iodine diffusion for three days at 1000°K,

half of each sample was washed with carbon tetrachloride and then placed in carbon tetrachloride for three weeks. The carbon tetrachloride was then decanted and the powder allowed to dry. The samples as taken from the tubes and those washed with carbon tetrachloride were analyzed for iodine content by neutron activation analysis. The concentrations of iodine measured for the samples taken from the tubes were 680, 150, and 665 ppm while the concentrations observed for the samples treated with carbon tetrachloride were 630, 80, and 460 ppm. No detectable quantity of iodine was measured for a DVT 1 sample that had not been exposed to iodine. These results indicate significant amounts of iodine were removed by the carbon tetrachloride wash and therefore had not diffused into the bulk of the polycrystalline material.

H. Tunnel Junction Fabrication and Equipment

Tunnel junctions of the form M/C/$NbSe_2$ where M=Pb or Sn and C=100-200 Å of graphite were prepared. Carbon barriers were evaporated from an electrode arrangement that was formed from emission spectrograph quality electrodes. In order to bring the current density required for carbon evaporation within the current capability of the filament transformer, the electrodes were machined to a smaller O.D. in the contact area. One electrode was machined with a 0.5 cm shoulder which terminated in a 20° conical tip. The mating electrode had a cylindrical cross section measuring 0.2 cm in O.D.

The electrodes were held in contact by a negator spring which applied a nearly constant force as the electrode length decreased with carbon evaporation. Counterelectrodes of tin were evaporated from a tungsten basket while lead electrodes were evaporated from a tantalum

cup heated by a tungsten filament. The carbon electrode assembly and the tungsten filament for evaporation of lead or tin were arranged in the vacuum chamber so that the graphite and metal counterelectrodes could be formed without breaking the vacuum. This was achieved by placing an aluminum shield between the electrode assemblies and using a magnetically controlled arm to properly locate the sample over each electrode assembly.

In some instances junctions were formed on the "as grown" crystal surfaces. In other cases the $NbSe_2$ crystals were cleaned in distilled acetone and distilled trichlorotrifluoroethane.

When Pb/C/Au junctions were formed, the gold surfaces were etched with a solution consisting of one part nitric acid, five parts hydrochloric acid, and 6 parts (v/v) water at a temperature of 315-325°K, followed by a boil in distilled water and a trichlorotrifluoroethane rinse.

After locating the sample on the stainless steel sample mount 8-10 cm above the carbon electrode assembly and after a pressure of $1x10^{-5}$ to $1x10^{-6}$ torr was reached, the carbon electrodes were outgassed at a low current of 10-20 A for approximately one to two minutes. The carbon barrier was formed by a series of evaporation and cooling cycles which were necessary to allow the electrode holder to cool and thus prevent overheating the sample. After the carbon layer appeared to be of the proper thickness, as indicated by its color*, the sample was rotated into a position above the tungsten filament to form the metal counter-

* A carbon thickness versus color scale was established by Milkove[28].

electrodes. A stainless steel mask which was fabricated with three rectangular openings was located just below the sample surface. The crossectional area of the openings was 0.015 cm^2. The alignment of the mask between the sample and the filament was such that three counter-electrodes could be formed within the boundaries of the carbon layer. In some cases the samples were not large enough to form more than one counterelectrode.

After the junctions were fabricated they were stored in a vacuum until they were installed in the multiprobe sample holder for analysis. Current versus voltage and dI/dV versus voltage curves were recorded for all tunnel junctions using a circuit described by Adler et al.[29] and shown in Figure 5.

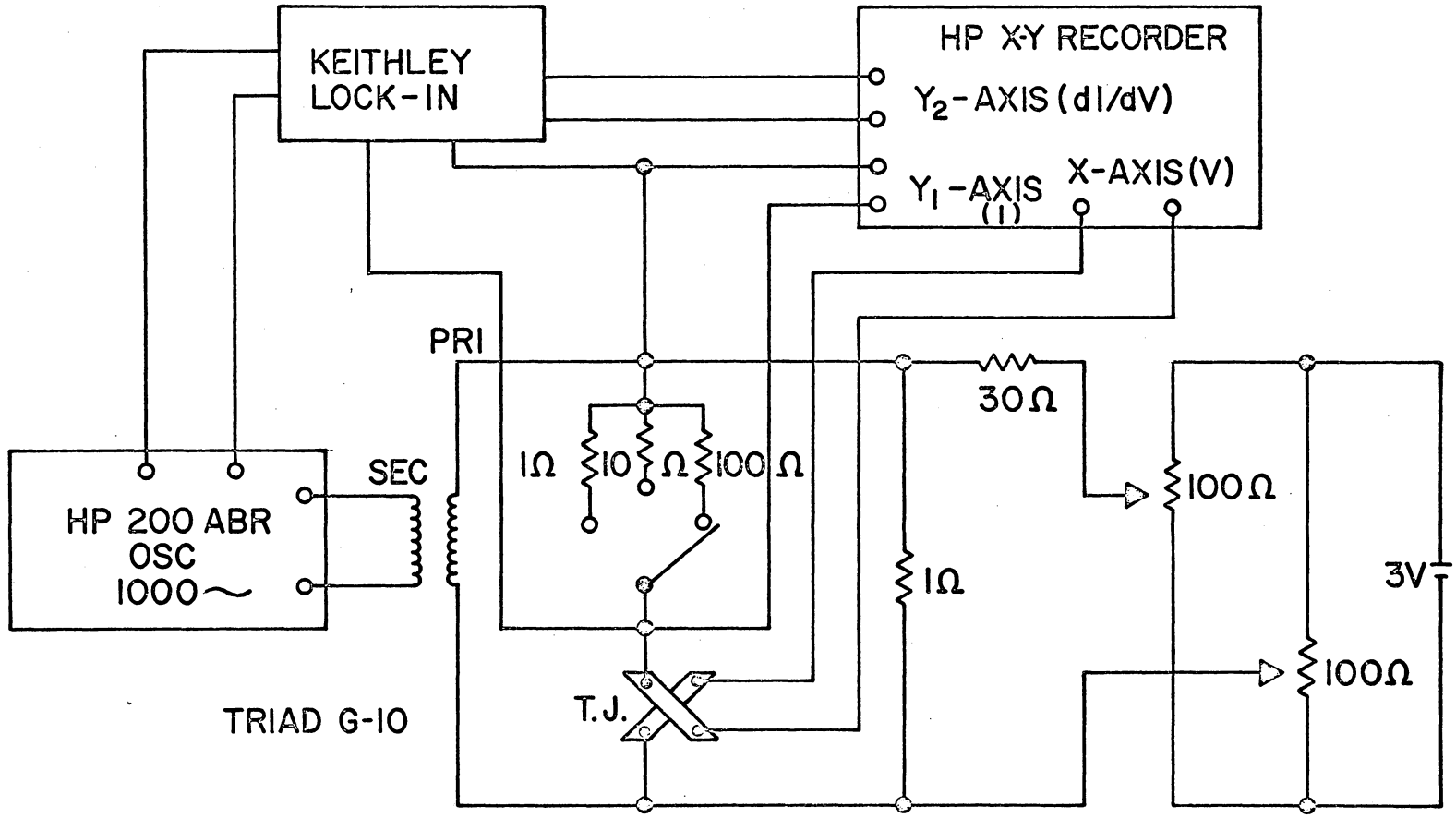

FIGURE 5. Circuit for Measuring Current Versus Voltage Characteristics of Tunnel Junctions (After J. G. Adler and J. E. Jackson[29]).

III. RESULTS AND DISCUSSION

A. Crystal Nucleation and Growth

The only differences in the preparation of DVT batches 1 and 2 were in the total time at 1200°K and in the anneal time at 1015°K. Variations in these times did not appear to affect the crystal yield or properties. As will be seen later, the transport properties of these two batches were very similar. In both cases the resulting growths consisted of masses of small single crystals intergrown and forming a cake throughout the bottom half of the tube with several larger platelet single crystals randomly distributed on top of the cake. Some crystals were observed to be growing suspended from the top of the tube and completely separated from the cake. The crystals were about 2×10^{-4} to 6×10^{-3} cm thick and up to 0.6 cm in length and width.

The preparation of DVT batches 3 and 4 was the first attempt to investigate the effect of deviations from stoichiometry. In this experiment DVT 3 was prepared as $NbSe_2$ and DVT 4 as $Nb_{0.97}Se_2$. Both batches were processed at the same time and DVT 3 served as a stoichiometry control. The single crystal yield and appearance on the interior of the tube for DVT 3 was similar to that described for DVT 1 and DVT 2. The most significant difference that readily could be observed for DVT 4 was that the cake had not remained in the bottom half of the tube but had been transported to the upper region of the tube and in general had an expanded appearance. The single crystals were intergrown in many cases and were crowded by the expanded charge. Needle-like crystals were also noted which have been described in the

literature as $NbSe_3$[2]. The overall appearance of DVT 3 and DVT 4 is shown in Figure 6. The principal differences in the time-temperature schedules for these two growths and growths DVT 1 and DVT 2 are in the total initial reaction time at 775-825°K and the time at 775-825°K after the first homogenization. The total time at the 775-825°K temperature level was shortened by a total of 6.5 days for DVT 3 and DVT 4.

Growths DVT 5 and DVT 6 were a continuation of the deviation from stoichiometry study. DVT 5, prepared as $NbSe_2$ and intended to be a control, was processed with DVT 6 which was prepared as $Nb_{0.95}Se_2$. The appearance of DVT 5 and the single crystal yield was much like the other growths prepared as $NbSe_2$, i.e., DVT 1, DVT 2 and DVT 3. DVT 6 had an appearance very similar to DVT 4, i.e., needle-like crystals in some areas and an expanded charge. DVT 6 had such a low single crystal yield that only one crystal was found that was large enough for transport measurements.

Growths 7 and 8 were prepared as $NbSe_2$ and $Nb_{.99}Se_2$, respectively. For these batches, the initial reaction time was limited to 3 days and the time after the first homogenization was 2 days. The time at 1200°K was 12 days followed by a 5 day anneal at 1025°K. DVT 7 had a high single crystal yield. The size and shape of the crystals and the location of the charge were similar to that of DVT 3 and DVT 5. Long needle-like crystals and expanded charge formed in DVT 8. The single crystal yield of DVT 8 was not as great as that of DVT 7. Transport measurements were made on previously grown samples while many of the new growths were being prepared. From these measurements it became apparent that the short initial reaction time and the time after first homogeni-

(a)

(b)

FIGURE 6. (a) Appearance of DVT 3 ($NbSe_2$) and DVT 4 ($Nb_{.97}Se_2$) Batches; (b) Appearance of Several DVT Batches Showing Effect of Selenium Concentration on Growth Conditions.

zation may have affected crystal properties. For this reason, DVT 7 and DVT 8 were not analyzed.

One attempt was made to prepare a growth which was rich in niobium. DVT 9 was originally prepared as $Nb_{1.05}Se_2$. After the completion of the schedule outlined in Table 1, crystal growth did not occur. The appearance of the powder was flat black as contrasted to the "sparkle" that the other growths had. Single crystals of 2H-$NbSe_2$ have mirror-like surfaces and when a cake is formed of many tiny crystallites it sparkles. It was decided to form stoichiometric $NbSe_2$ with half of this charge by adding the proper quantity of selenium and repeating the growth process. After these operations, single crystals of 2H-$NbSe_2$ formed.

Figure 6 is a pictorial summary of the effect that selenium has upon the growth of 2H-$NbSe_2$ by the DVT procedure. DVT 6 ($Nb_{.95}Se_2$) and DVT 4 ($Nb_{.97}Se_2$) show the expanded charge and the crowded condition that developed as the selenium concentration approached stoichiometry. DVT 3 ($NbSe_2$) shows the single crystals distributed throughout the tube and the charge remaining in the bottom half of the tube. DVT 9, shown as $Nb_{1.05}Se_2$, shows the flat black appearance of this composition. DVT 9, shown after the composition was adjusted to $NbSe_2$, shows the "sparkle" that is typical of the other DVT growths having a chemical composition of $NbSe_2$.

The mechanism of crystal growth by the DVT method is not completely understood at the present time. It does appear that the relative selenium and niobium concentrations are important. In the case of DVT 9 where the niobium concentration was in excess of stoichiometric pro-

portions, growth did not occur but did occur after the proper amount of selenium was added to the charge to bring it to stoichiometric proportions. These results, when considered with the transport effects that occurred when the selenium concentration was in excess of stoichiometry (DVT 4 and DVT 6), indicate that selenium acts as a transporter. A high degree of crystal perfection, as indicated by the RRR values of 133 to 140, was observed for crystals from growths DVT 1 and DVT 2. One known difference between these and other growths which yielded crystals with RRR values of 19 and 21 was longer initial reaction times. Longer initial reaction times allow the selenium to be more thoroughly reacted with the niobium and thus results in a lower selenium pressure before the charge is taken to a higher temperature for crystal growth.

In the chemical transport procedure described by Nitsche et al.[21], considerable attention is placed upon $\dot{m}$, the amount of material arriving in the growth chamber per unit time. Nitsche indicates that whem $\dot{m}$ exceeds a critical value, the growing seeds cannot digest the arriving materials and supersaturation will increase until additional nucleation occurs. This can result in polynucleation and the intergrowth of crystals. By analogy, it is believed that in the DVT procedure the degree of supersaturation, which is determined by the amount of unreacted selenium, not only determines whether growth will occur, but also determines the rate of growth and the degree of crystal perfection.

B. Crystal Characterization

1. X-Ray Diffraction

X-ray diffraction measurements performed on crystals from the IVT 1, DVT 1, and DVT 2 growths indicated all were in the 2H layer modifi-

cation. Unit cell dimensions along the C-axis were measured as 12.552 Å, 12.562 Å, 12.454 Å, and 12.558 Å for IVT 1A, IVT 1B, DVT 1A, and DVT 2A respectively. These values are in relatively good agreement with the value of 12.54 Å given by Revolinsky et al.[2].

Back scattering and transmission Laue photographs were prepared for several IVT and DVT crystals. In all cases the photographs were made with the x-ray beam perpendicular to the basal plane. The sixfold symmetry of the lattice for DVT 1C and IVT 1C crystals is readily apparent from back-scattering patterns presented in Figure 7. Similar back-scattering Laue patterns were observed for other IVT and DVT crystals.

Several transmission Laue patterns were prepared to compare structural defects in both types of crystals. This analysis involved preparing Laue patterns for several DVT and IVT crystals as well as preparing Laue patterns for different sections of each crystal. These results are summarized in Figures 8 and 9. The amount of asterism shown in these patterns and the variations in asterism from one section of a crystal to another indicates structural defects are present. The elongation of a Laue spot is normally associated with a crystal plane that has been bent or otherwise distorted. IVT 1C was cleaved from a larger crystal and could easily have been bent during this preparation. DVT 1C was characterized "as grown", yet shows as much variation in asterism from one section of the crystal to another as IVT 1C. It is therefore believed that some of the asterism is a result of layer misorientation that occured during growth. Antonova et al.[9] associate the diffusion and elongation of the points on Laue patterns of 2H-$NbSe_2$, grown by the

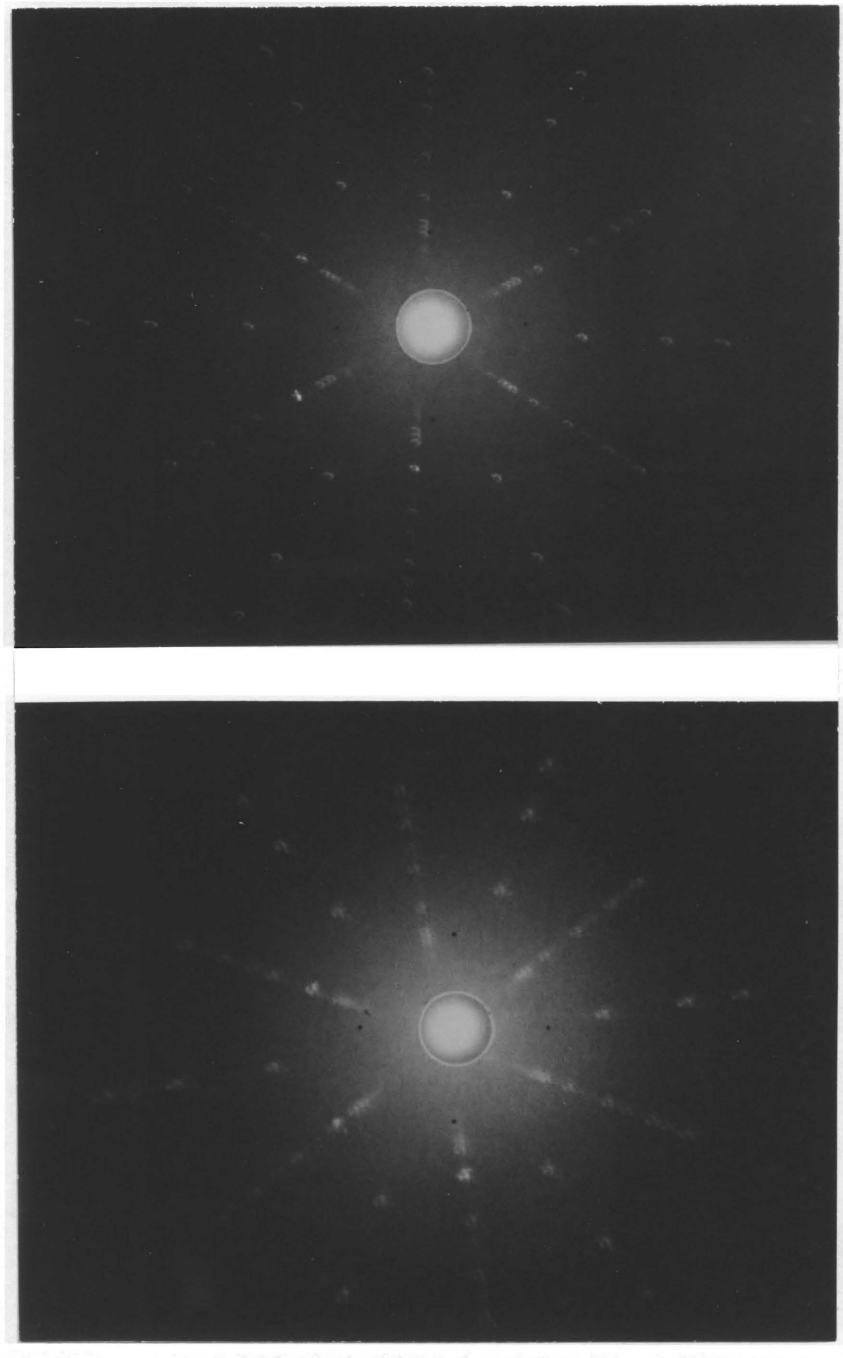

FIGURE 7. Back-reflection Laue Photographs of DVT 2B and IVT 1C Crystals (3-cm crystal-to-film distance).

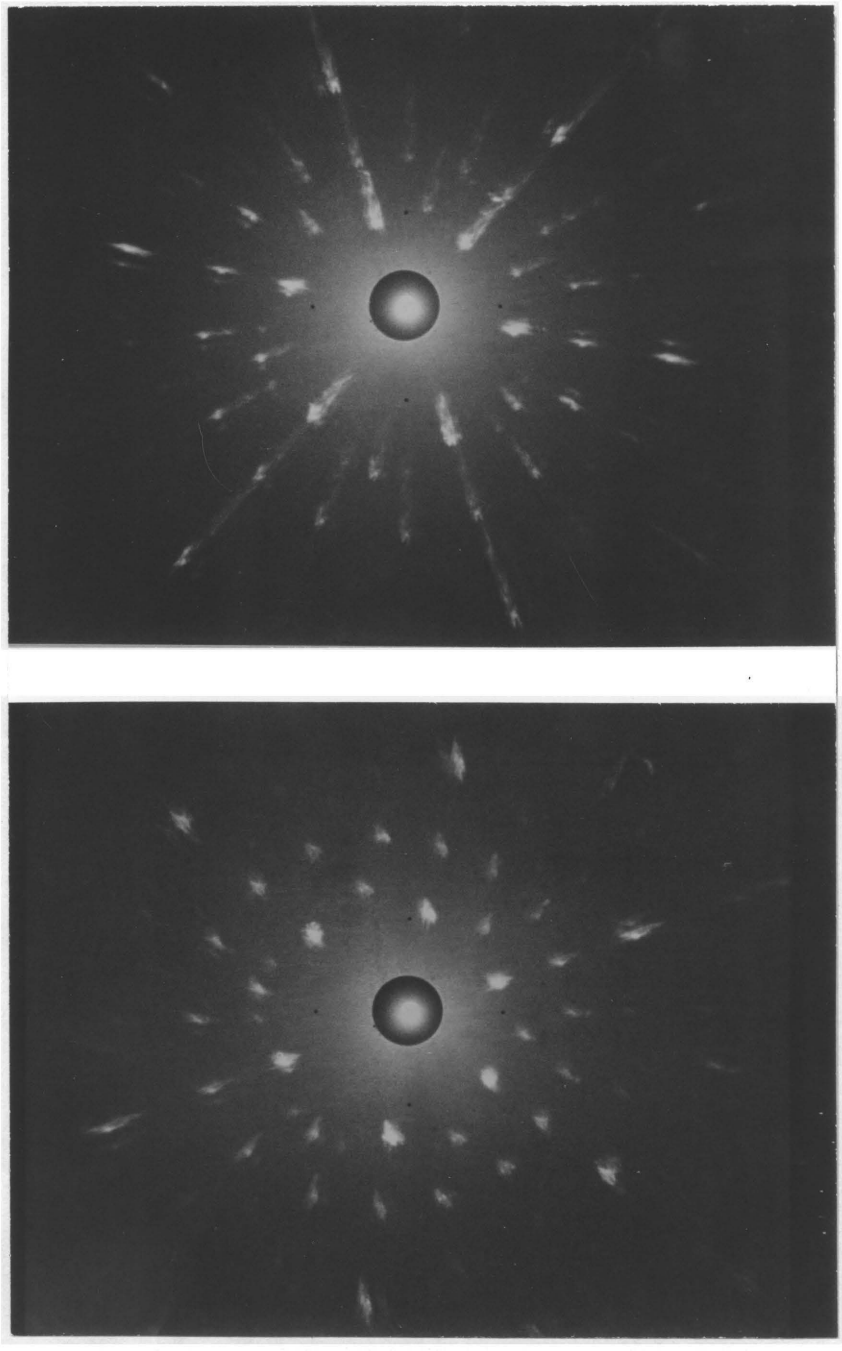

(a)

(b)

FIGURE 8. Transmission Laue Photographs of Sections of DVT 1C (a) Point Near Edge of Crystal; (b) Midpoint of Crystal (3-cm crystal-to-film distance).

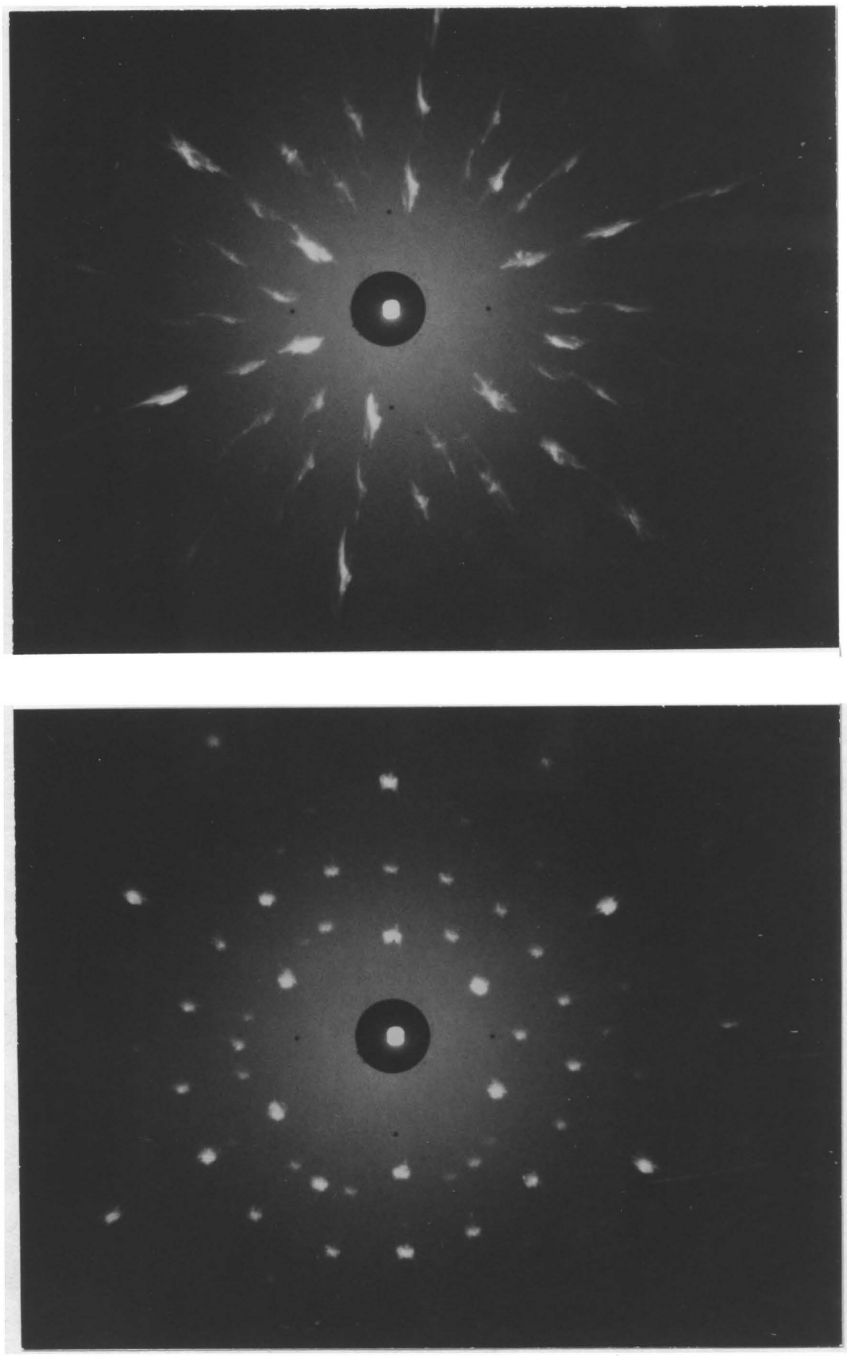

(a)

(b)

FIGURE 9. Transmission Laue Photographs of Two Sections of IVT 1C (a) Point Near Edge of Crystal; (b) Midpoint of Crystal (3-cm crystal-to-film distance).

chemical vapor transport method, with a double layer misorientation resulting from a shifting of layers in planes parallel to the basal plane.

The RRR values observed for DVT 1C and IVT 1C were 137 and 41 respectively. A correlation between these values and the defect structure shown in Figures 8 and 9 does not appear to exist. This is an indication that the RRR value for a crystal is influenced more by the intralayer structure than the interlayer structure.

2. X-Ray Photoelectron Spectroscopy

In order to characterize the surface of $NbSe_2$ samples, core and valence electron binding energies for niobium and selenium were measured. XPS spectra were measured for DVT crystals representing different transport properties and growth conditions. Data were taken on three crystals from the IVT growth.

Measurements of the niobium core levels on the "as grown" faces of IVT 1A indicate the surface constitution is predominantly oxidized niobium (Figure 10). The chemical composition is most likely $NbSe_2$ although the possibility of surface niobium oxides cannot be ruled out. The XPS spectra reveal that the surface composition of a freshly cleaved IVT 1A is primarily elemental niobium. The identification of Nb° was accomplished by comparison of the binding energies of this work with the value reported by McGuire et al.[30]. The XPS data from this work and that by McGuire et al. have been included as Tables II and III, respectively. IVT 1B and IVT 1C were cleaved from larger crystals and therefore could not be characterized "as grown". The cleaved surface of IVT 1B and IVT 1C are very similar to that of IVT 1A. (The spectrum of IVT 1C is not shown in Figure 10.) In cleaved IVT 1B there is some

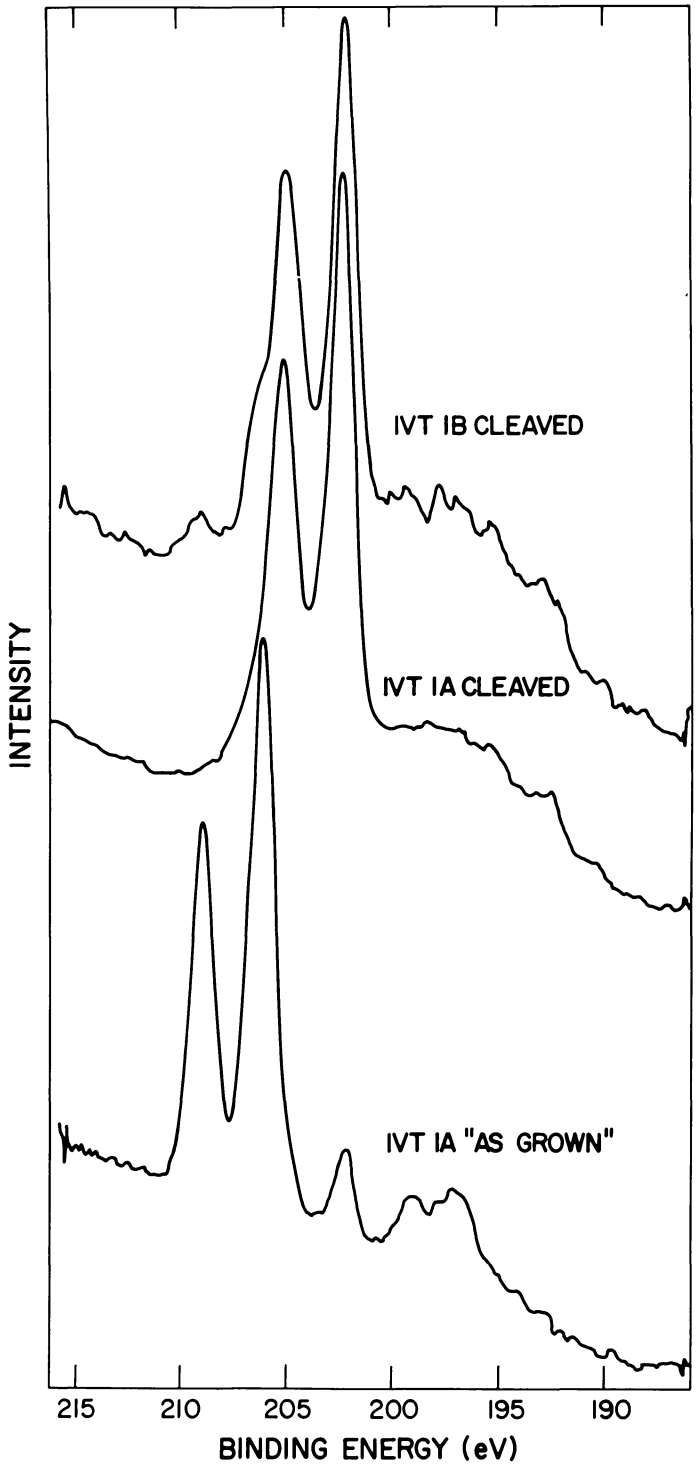

FIGURE 10. Photoelectron Spectrum of Nb° $3d_{5/2}$, Nb° $3d_{3/2}$, Nb^{4+} $3d_{5/2}$, and Nb^{4+} $3d_{3/2}$ Levels in 2H-$NbSe_2$.

TABLE II. BINDING ENERGIES (eV) FOR NIOBIUM IN 2H-$NbSe_2$

CRYSTAL	Nb° $3d_{3/2}$	Nb° $3d_{5/2}$	Nb^{4+} $3d_{3/2}$	Nb^{4+} $3d_{5/2}$
DVT 1C				
"As Grown"	205.5	202.5	209.4	206.5
DVT 2B				
"As Grown"	205.5	202.3	209.2	206.3
DVT 4A				
"As Grown"	205.3	202.6	209.6	
Cleaved	205.4	202.7	209.5	
DVT 5B				
"As Grown"		202.6	209.2	206.2
Cleaved	205.0	202.2		
IVT 1A				
"As Grown"			209.1	
Cleaved	205.2	202.0		206.1
IVT 1B				
Cleaved	205.0	202.2	209.1	
IVT 1C				
Cleaved	205.1	202.3	209.2	
σ	0.21	0.23	0.094	0.14

TABLE III. BINDING ENERGIES (eV) GROUP Vb COMPOUNDS. DATA FROM McGUIRE ET AL.[30]

COMPOUND	Nb $3d_{5/2}$	COMPOUND	Nb $3d_{5/2}$
Nb	202.3	$KNbO_3$	206.7
NbS_2	207.9	Nb_2O_5	207.6
NbN	207.5	K_2NbF_7	209.3
$NbBr_5$	207.3	NbF_5	209.6
$NbCl_5$	208.2		

evidence of the presence of higher oxidation states of niobium as shown by the small peak at about 209 eV and the shoulder on the Nb $3d_{3/2}$ peak at about 206 eV. The appearance of the Nb 4d peak at about 14 eV in the valence region confirms the results observed for the 190-220 eV region (Figure 11).

The appearance of the Nb° peak after cleaving appears to be consistent with the x-ray data of Kadijk et al.[31] which indicates that the 2H-$NbSe_2$ structure can accommodate a considerable proportion of additional niobium atoms on octahedral interstices (See Figure 1 for structure.) However, it does not seem reasonable that there would be sufficient niobium atoms on these sites to virtually screen the niobium atoms in the Nb^{4+} state which are located between the selenium sheets. Assuming that the escape depth of the ejected photoelectrons is 10-15 Å, then it would appear that more electrons from atoms in the Nb^{4+} state, which are separated from the Nb° atoms in the van der Waals gap by about 6 Å, should have been observed. One possible interpretation of this result is that the $Nb_{1+x}Se_2$ α phase, identified by Revolinsky et al.[2] is present. It was reported that the phases between NbSe and $NbSe_2$ appear to be based on the $NbSe_2$ structure. If this is the case, the niobium in this compound could exist in the Nb^{2+} oxidation state. The binding energies for Nb^{2+} may be close to Nb° although no data could be found to confirm this.

An examination of the niobium core levels in the DVT 1C and DVT 2B crystals shows that both elemental niobium and oxidized niobium ($NbSe_2$) are present (Figure 12). The spectrum is characterized by two well

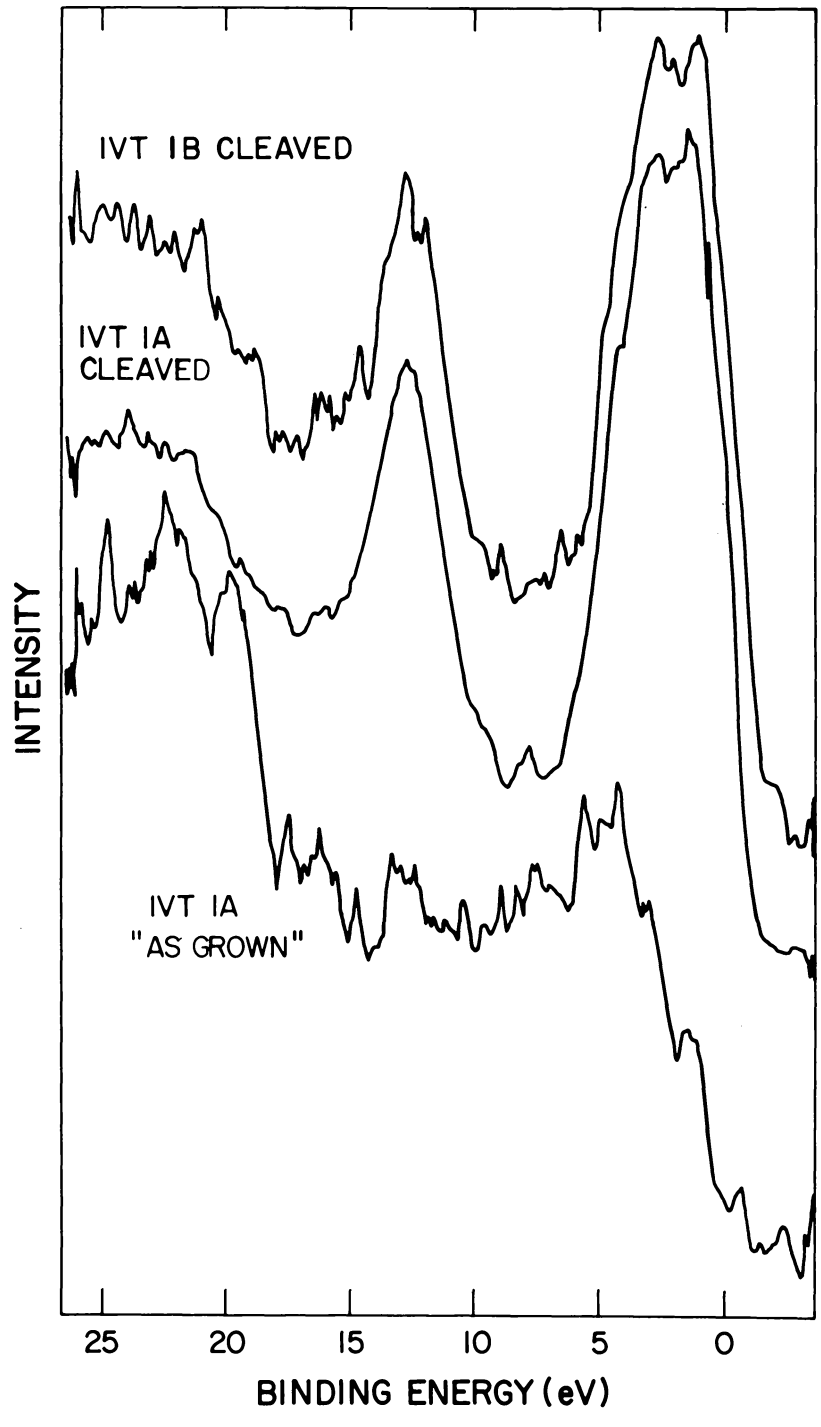

FIGURE 11. Photoelectron Spectrum of Nb 4d Level in 2H-$NbSe_2$.

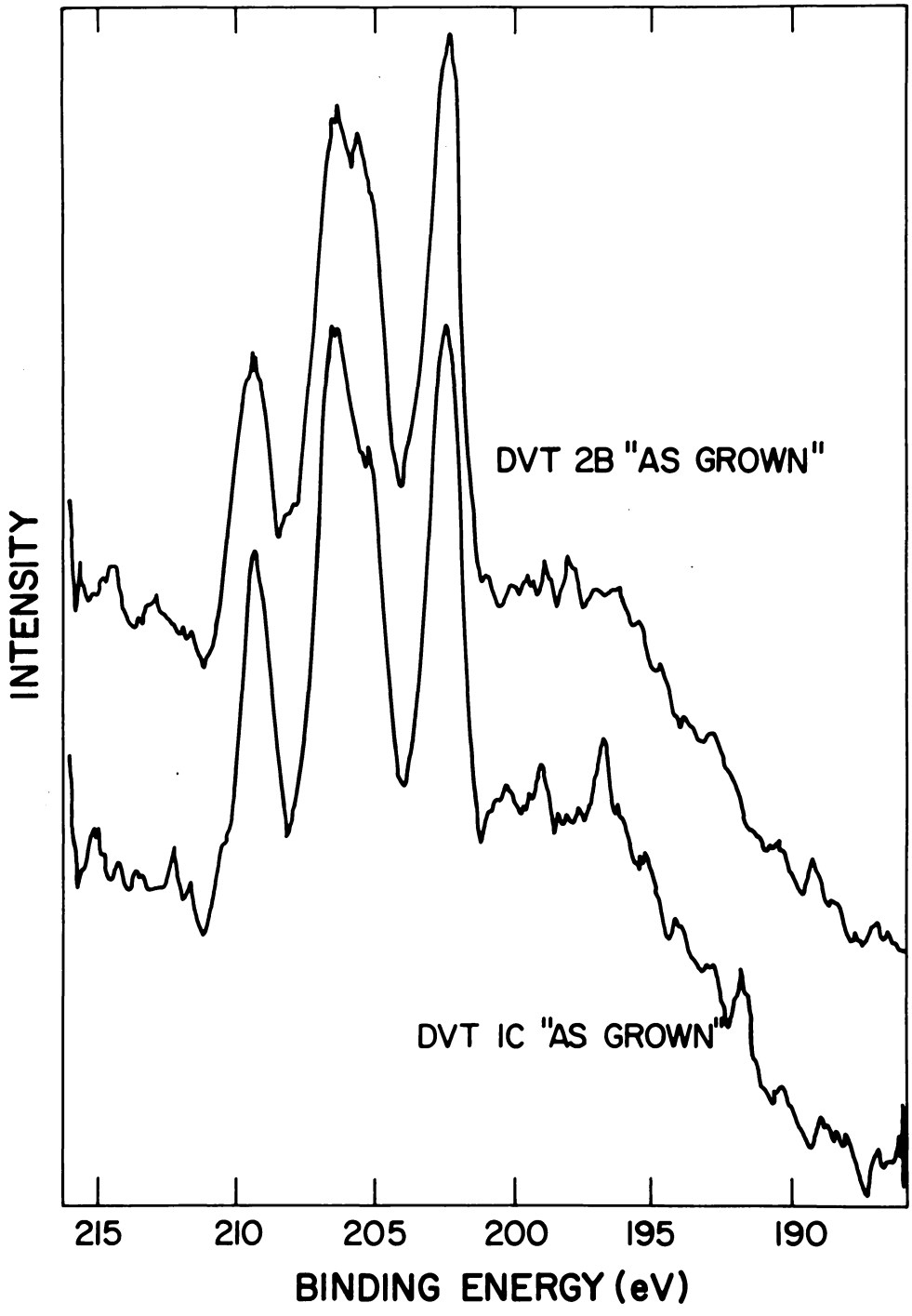

FIGURE 12. Photoelectron Spectrum of Nb° $3d_{5/2}$, Nb° $3d_{3/2}$, Nb^{4+} $3d_{5/2}$, and Nb^{4+} $3d_{3/2}$ Levels in 2H-$NbSe_2$.

resolved single peaks at the highest and lowest binding energies corresponding to Nb^{4+} (Nb $3d_{3/2}$) and Nb° (Nb $3d_{5/2}$) respectively, and an unresolved pair of peaks at about 207 eV. The unresolved peaks correspond to Nb^{4+} (Nb $3d_{5/2}$) on the high energy side of the peak and Nb° (Nb $3d_{3/2}$) on the low energy side. Scans of the valence region show the Nb 4d peak at about 14 eV (Figure 13). It is evident from the XPS measurements that the surface of these DVT crystals is chemically unlike that for the IVT crystals.

After the "as grown" surfaces of DVT 1C and DVT 2B were studied with XPS, a decision was made not to cleave them because they were thinner and more delicate than the IVT crystals. As this work progressed and variations in T_c and RRR values for crystals from different growths were observed it became necessary, for correlation purposes, to cleave the DVT crystals for XPS studies. However, DVT 2B had been accidentally destroyed and DVT 1C had been doped with iodine. Therefore, the cleaving experiment was performed on other crystals selected from growth DVT 1 which represented crystals of high RRR (133) and a typical T_c (7.1°K) for 2H-$NbSe_2$. XPS spectra of the "as grown" surface of these crystals were very much like that of DVT 1C and DVT 2A while the spectra for the cleaved surfaces were very similar to those observed for cleaved IVT crystals.

XPS spectra were measured for a crystal from DVT 5 growth which represented crystals of low RRR (21) and depressed T_c (6.59°K). XPS spectra measured before and after cleaving DVT 5B revealed that the "as grown" surface was typical of all other DVT crystals analyzed and that the cleaved surface is very much like the IVT and other DVT crystals

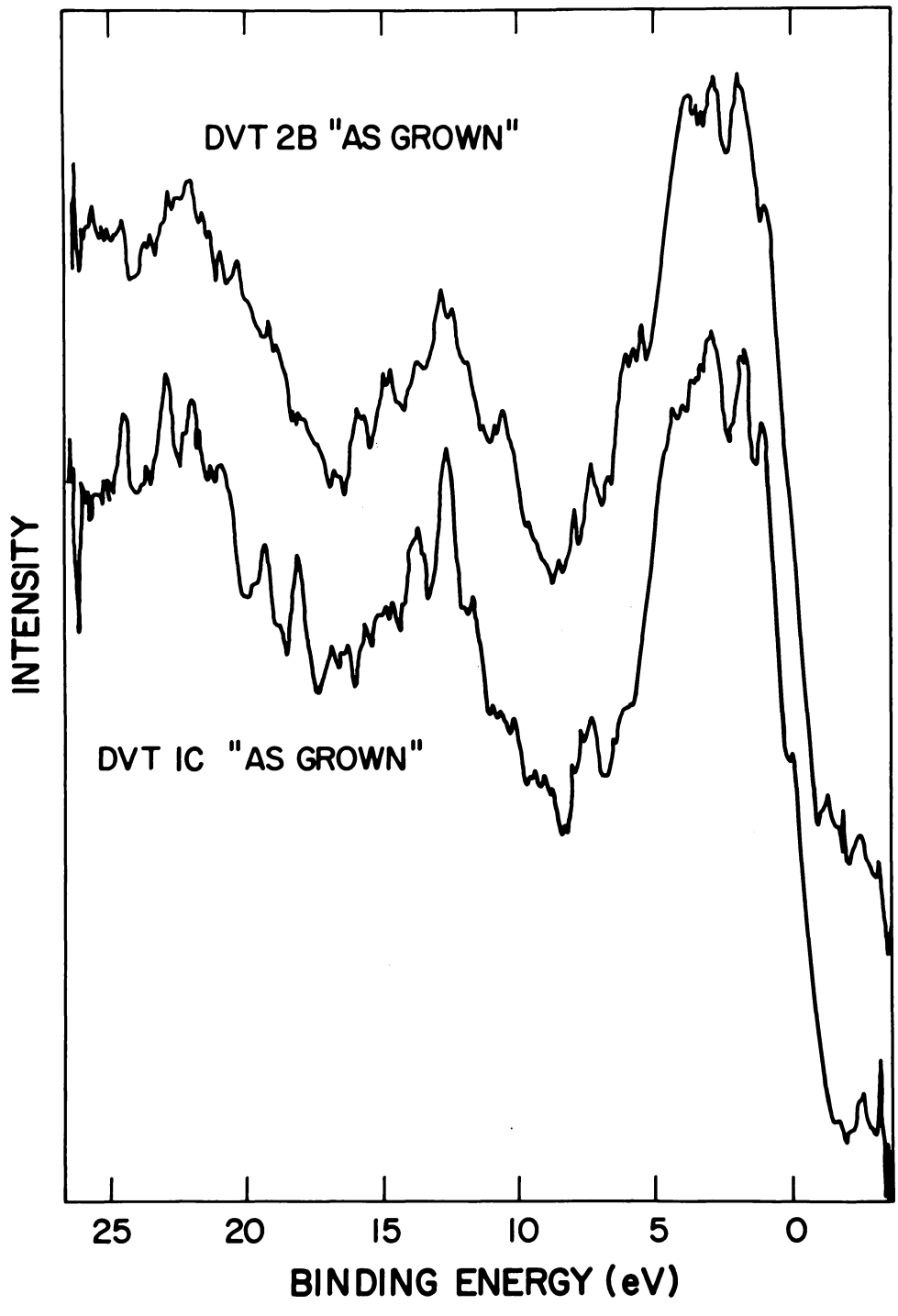

FIGURE 13. Photoelectron Spectrum of Nb 4d Level in 2H-$NbSe_2$.

(Figure 14).

An observation that has been common to all cleaved IVT and DVT crystals discussed thus far is that the cleaved surface appears to be primarily elemental niobium or a very low oxidation state of niobium. Prior to the analysis of the crystal from growth DVT 4, which is rich in selenium, it was speculated that the niobium on the cleaved surface would be more thoroughly oxidized by the excess selenium. The XPS spectrum for the "as grown" surface shows smaller Nb^{4+} $3d_{3/2}$ and Nb^{4+} $3d_{5/2}$ peaks than that observed for any of the other IVT or DVT crystals (Figure 15). The cleaved surface is primarily elemental niobium with a detectable quantity of the Nb^{4+} oxidation state. However, these peaks do not appear to be any larger than those observed on the cleaved surface of IVT 2 (Compare Figure 10 to Figure 15.) Therefore, it does not appear that excess selenium brings about a more complete oxidation of niobium.

Neutron activation analysis indicated the level of iodine in the IVT crystals was 400-700 ppm. To determine the chemical form of iodine in these crystals, the photoelectron spectrum of the iodine $3d_{3/2}$ level was measured for IVT 1C powder. IVT 1C was chosen for this work because it had a higher iodine content than IVT 1A. IVT 1C had previously been cleaved from a larger crystal and therefore any iodine found would be more representative of the bulk rather than an "as grown" surface. The first XPS analysis was performed on a layer cleaved from IVT 1C but no iodine was detected. A cleaved layer was ground to increase the surface area and the powder dusted on sticky tape. The resulting XPS spectrum is shown in Figure 16. A binding energy of 629.6 eV was measured.

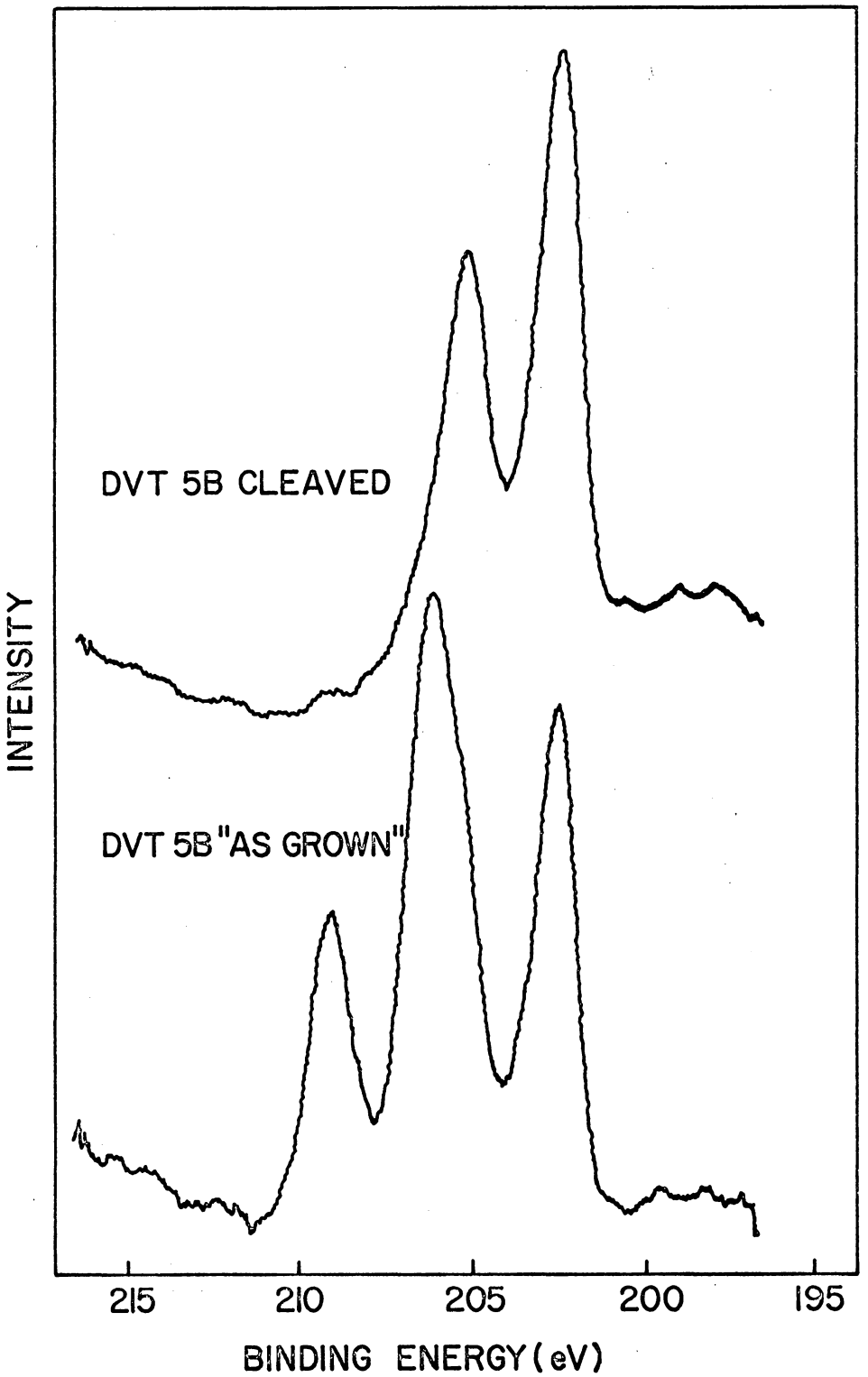

FIGURE 14. Photoelectron Spectrum of Nb° $3d_{5/2}$, Nb° $3d_{3/2}$, Nb^{4+} $3d_{5/2}$, and Nb^{4+} $3d_{3/2}$ Levels in 2H-$NbSe_2$.

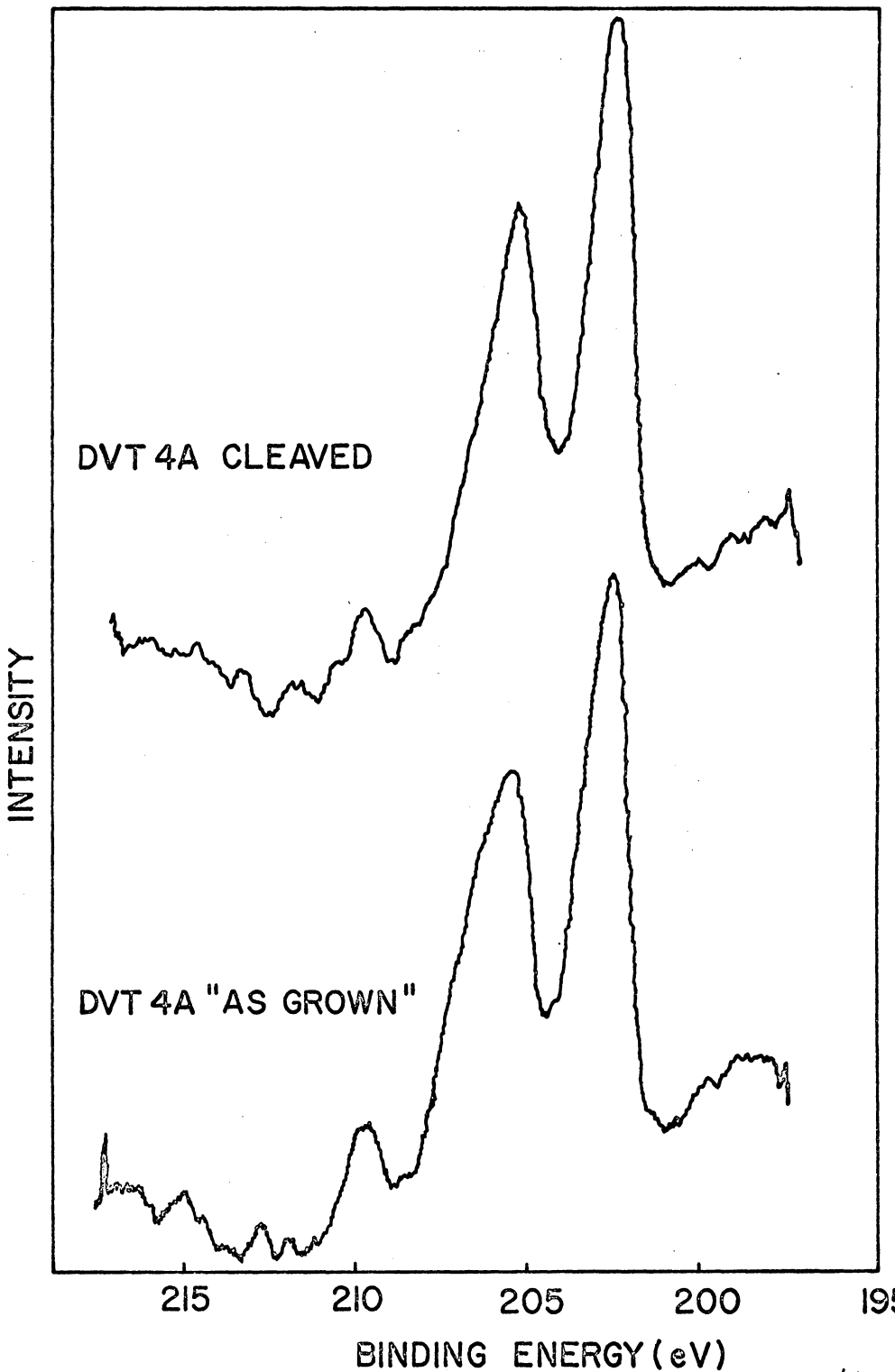

FIGURE 15. Photoelectron Spectrum of Nb° $3d_{5/2}$, Nb° $3d_{3/2}$, Nb^{4+} $3d_{5/2}$, and Nb^{4+} $3d_{3/2}$ Levels in 2H-$NbSe_2$.

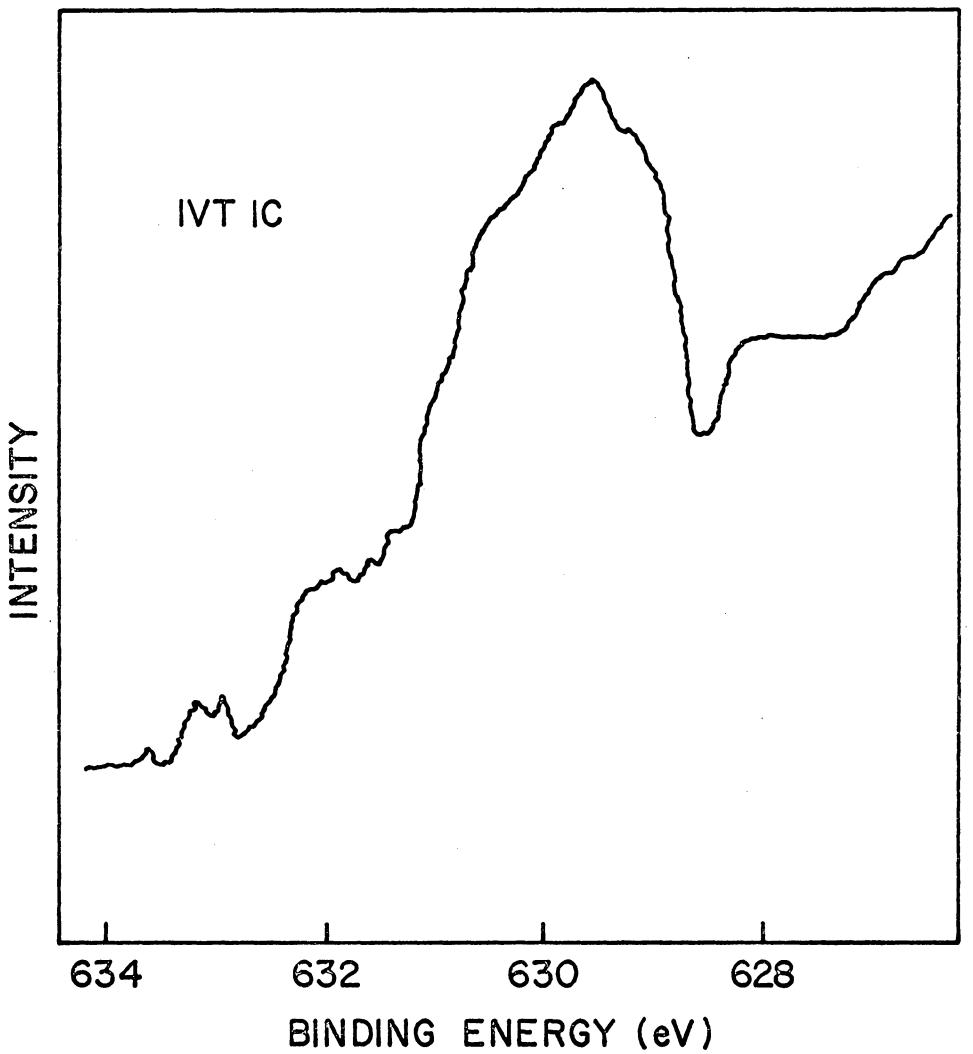

FIGURE 16. Photoelectron Spectrum of I $3d_{3/2}$ Level in 2H-$NbSe_2$ Grown by Iodine Vapor Transport.

This value is slightly lower than that reported for iodine in Group IIb iodines[27] and for potassium iodide[32]. However, the measured binding energy value is consistent with the existence of iodine in $NbSe_2$ as iodide ion. The differences between the binding energies reported here and those reported earlier[27,32] could be due to the lattice potential at the iodide site in $NbSe_2$ which would affect the measured binding energy[32].

C. Low Temperature Measurements

Transition temperatures, which were chosen as the midpoint of the temperature versus voltage curves, were measured as a function of an apparent current density. Transition temperatures at zero current density were determined from least squares fits of the J vs T_c^2 data. The dependence of T_c on J for several DVT and IVT crystals is shown in Figures 17 and 18. When these data and the data in Table IV are examined, three observations can be made:

(1) There exists a stronger dependence of T^2 upon current density for IVT 1A and IVT 1C than any of the other crystals.

(2) Two distinct groupings for the DVT crystals have occurred; one group, consisting of crystals from DVT batches 1, 2, and 9, having T_c values near 7.05°K and one group, consisting of crystals from DVT batches 3, 4, 5, and 6, having T_c values near 6.6°K.

(3) A summary of the T_c data in Table IV shows that of all the crystals evaluated, the T_c values for the DVT's were never higher than any of the values for the IVT's.

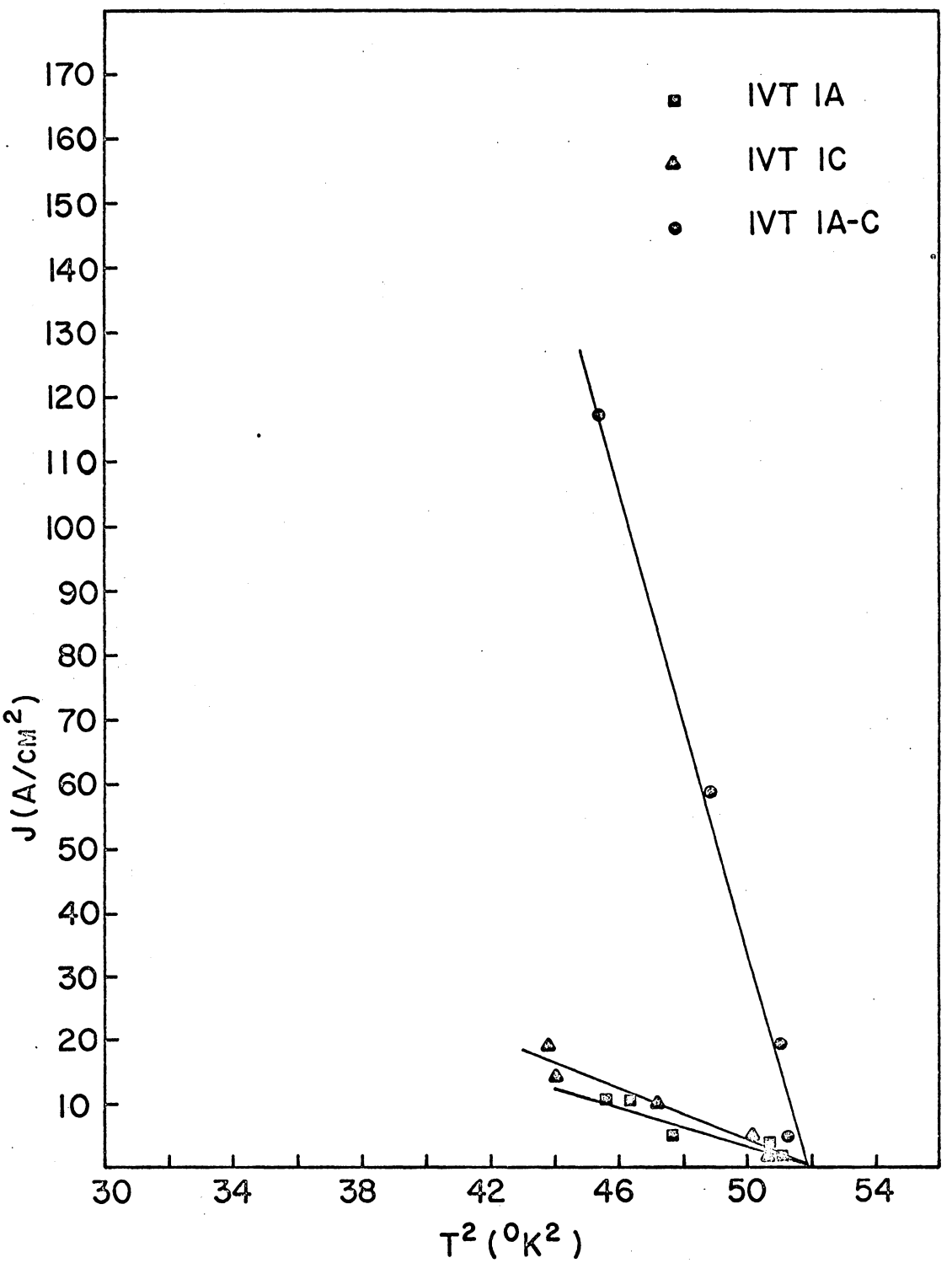

FIGURE 17. Transition Temperature of 2H-$NbSe_2$ at Different Current Densities (IVT).

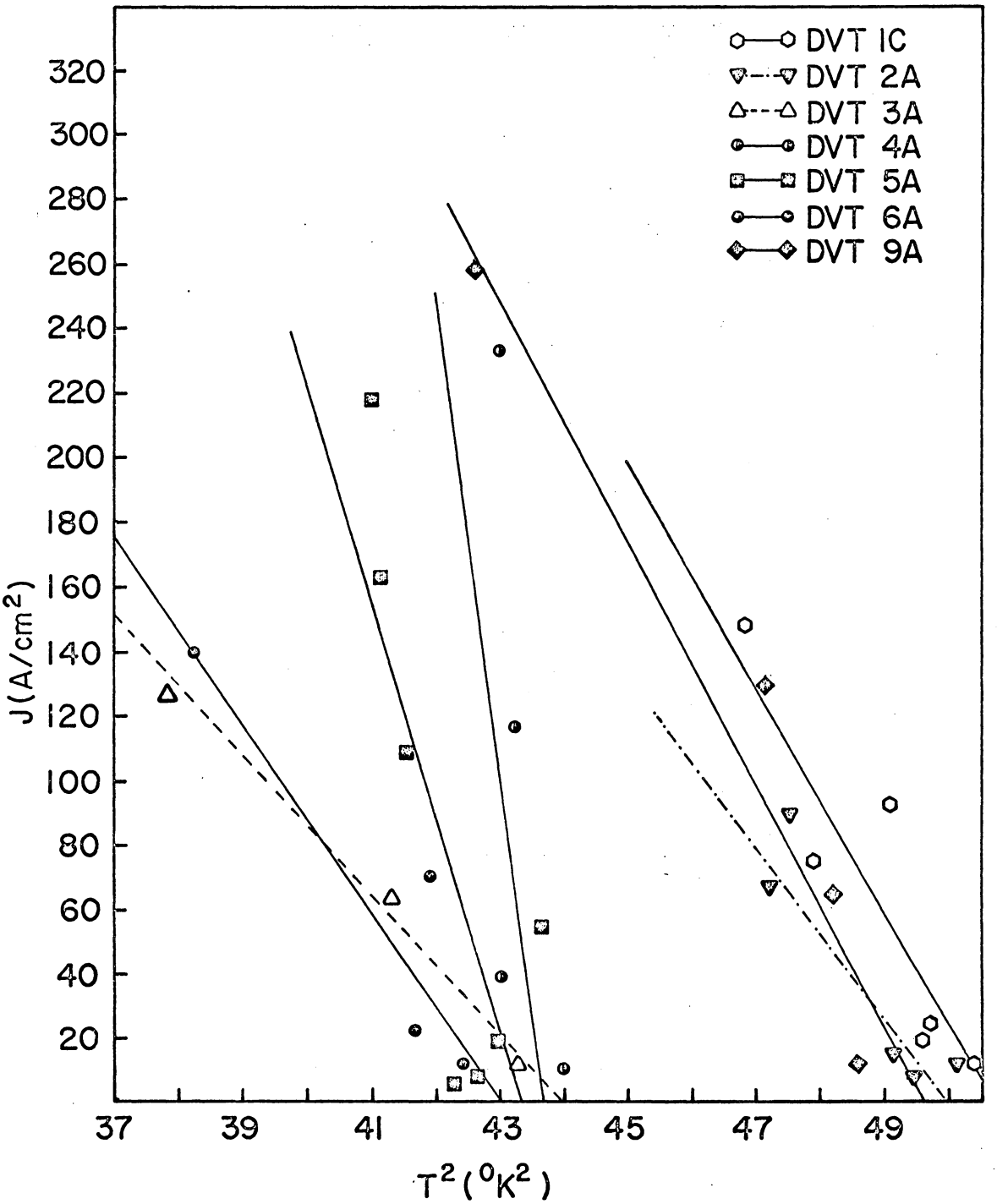

FIGURE 18. Transition Temperature of 2H-$NbSe_2$ at Different Current Densities (DVT).

TABLE IV. TRANSITION TEMPERATURE (T_c), RESIDUAL RESISTANCE RATIO (RRR), CRITICAL CURRENT (J_c) AND THICKNESS (t) DATA

CRYSTAL	CHEMICAL FORMULA	T_c(°K)	RRR	J_c(A/cm^2)	t(cm)
DVT 1A	$NbSe_2$	7.04	133		
DVT 1C	$NbSe_2$	7.12	137	1780	3.4×10^{-4}
DVT 2A	$NbSe_2$	7.07	140	1340	1.3×10^{-3}
DVT 2B	$NbSe_2$	7.05	133		
DVT 3A	$NbSe_2$	6.64	21	913	1.1×10^{-3}
DVT 4A	$Nb_{.97}Se_2$	6.61	21	6550	6.0×10^{-4}
DVT 5A	$NbSe_2$	6.59	21	2892	1.0×10^{-3}
DVT 6A	$Nb_{.95}Se_2$	6.56	19	1245	1.0×10^{-3}
DVT 9A	$NbSe_2$	7.05	54	1865	1.4×10^{-3}
IVT 1A	$NbSe_2$	7.24	39	80	1.0×10^{-2}
IVT 1A-C	$NbSe_2$	7.20	36	950	2.0×10^{-3}
IVT 1B	$NbSe_2$	7.14	42		
IVT 1C	$NbSe_2$	7.20	41	110	5.0×10^{-3}

[a] Chemical formula based on starting weights of Nb and Se.

[b] T_c at zero current density. T_c for DVT 1A, DVT 2B and IVT 1B was determined at a single current density.

[c] RRR was determined for currents flowing parallel to the layers.

These three observations will be treated in detail in the material that follows.

1. The Dependence of Critical Current Density on Crystal Thickness

An examination of the thickness data given in Table IV shows that IVT 1A and IVT 1C are much thicker than the DVT crystals. It has been demonstrated by Kopp et al.[26] that an inverse relationship exists between critical current density and thickness for cleaved IVT crystals. After examining the data by Kopp et al.[26], it was decided that IVT 1A would be cleaved and a J vs T_c^2 curve prepared for this thinner crystal which has been identified as IVT 1A-C. The dependence of T_c^2 upon current density for the crystal was observed to be much less than that of IVT 1A.

Kopp et al.[26] associated the $J \propto t^{-1}$ dependence with a surface pinning effect. They applied the theory of Kim and Stephen[33] to arrive at an expression of the form:

$$\frac{J_{cf}\,\phi_0}{c} = \frac{F_s}{t} + nF_v \qquad (5)$$

where $J_{cf}\,\phi_0/c$ is the magnetic force per unit length on a flux line, ϕ_0 is the flux quantum, c the speed of light, t the length of flux line, F_s a surface pinning force and F_v an interior pinning force. From this expression a current independent of thickness is predicted for thick crystals while a $J_{cf} \propto t^{-1}$ dependence holds for thin crystals. In the work by Kopp et al.[26] the critical current density J_{cf} was determined from the current versus magnetic field characteristics and the crossectional area of each crystal which was calculated from resistivity data.

The data of Kopp et al.[26] are presented in Figure 19 along with

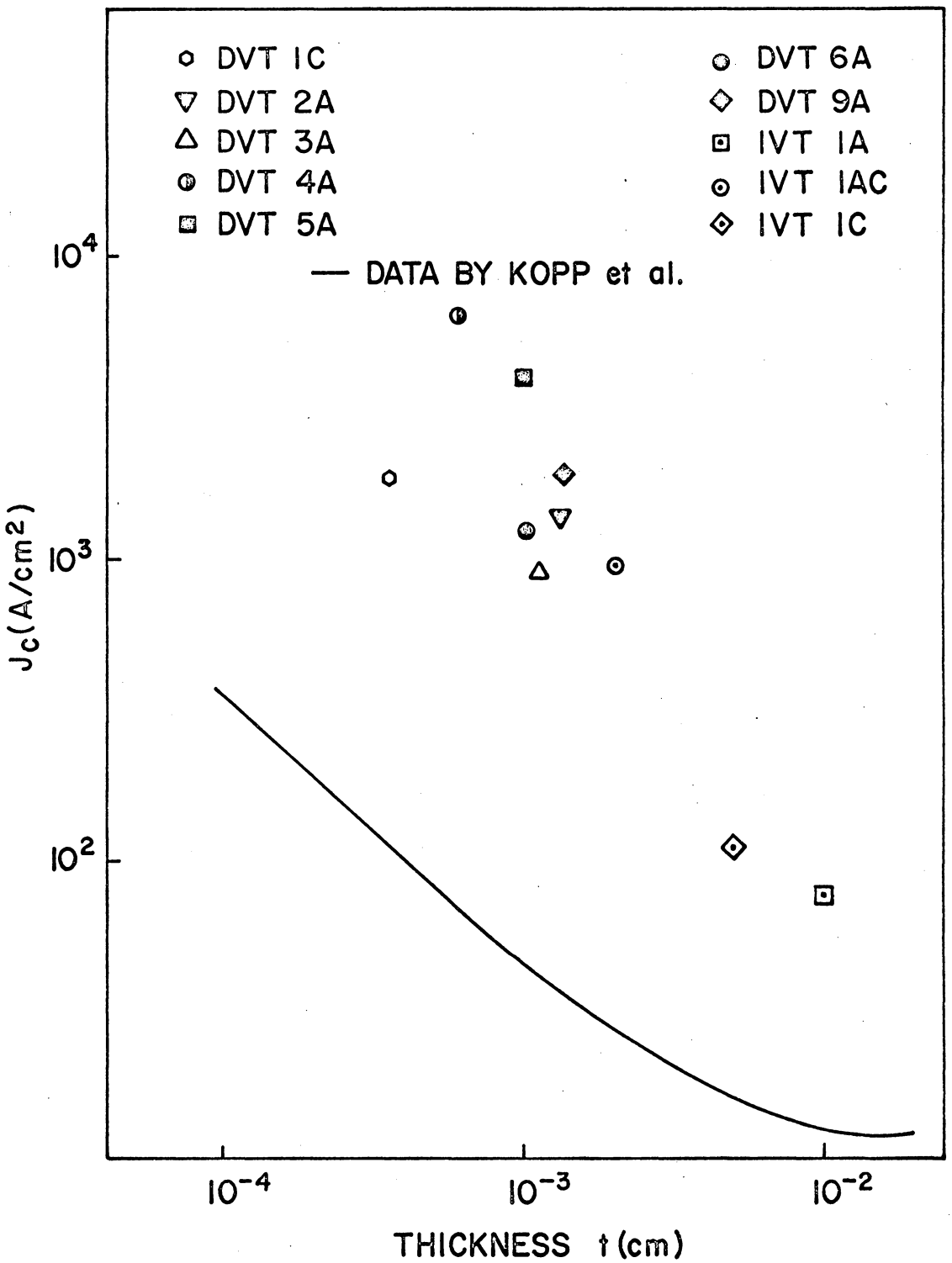

FIGURE 19. Effect of Thickness on Critical Current Density for Samples of 2H-$NbSe_2$ (DVT and IVT).

the data compiled for DVT and IVT crystals. There are basic experimental differences in the way these data were collected and therefore a direct comparison is not intended. Kopp et al.[26] determined J_{cf} in the presence of magnetic fields that ranged from 8 to 16 kOe. The critical currents for the IVT and DVT crystals were determined in zero field and have been defined as the current density intercept on a graph of J vs T_c^2 (Figures 17 and 18). This difference explains the one or two orders of magnitude higher current densities observed for the DVT and IVT crystals than their data. They indicated that the zero field critical current densities for the samples they evaluated were one to two orders of magnitude higher than those shown in Figure 19. Combining data from DVT crystals representing different growth conditions, which could have introduced different surface defects, along with data from IVT samples has possibly introduced scatter in the data. Even though these differences exist, the inverse relation with thickness can be seen in the data. Thus the higher critical current densities observed for some of the DVT samples are most likely related to sample thicknesses. However, limited critical field measurements made on DVT and IVT samples have indicated that the DVT's may possess higher Hc_2 fields[34] than the IVT's.

2. Superconducting Transition Temperatures and Chemical Composition

It is believed that the grouping of the T_c data for the DVT samples, the second observation, is related to growth conditions (Figure 18). As previously discussed growths DVT 1 and DVT 2 underwent longer initial reaction times than other growths. Samples from these growths appear to have fewer structural defects than others as evidenced by their high RRR values. Although the growth history of DVT 9 is dif-

ferent than that of DVT 1 and DVT 2 it can be characterized as having a long initial reaction time. The RRR value of 54 observed for DVT 9A was higher than any other DVT samples with the exception of crystals from growths DVT 1 and DVT 2. The reference to RRR values at this point is not being made to imply that high RRR results in high T_c, but is an indicator of growth conditions. Those crystals grouped around the T_c value of 6.6°K represent different growth conditions. All have a shorter initial reaction time than those referred to above. In addition to this DVT 4 and DVT 6 were prepared in a selenium rich atmosphere which results in intergrowth between crystals and a possible higher concentration of defects.

When a transition temperature less than 7°K is observed for 2H-$NbSe_2$ it is normally attributed to a deviation from stoichiometry. This interpretation stems from the works of Revolinsky, et al.[2] and Antonova et al.[7]. Revolinsky et al.[2] have shown that as the chemical composition goes from $NbSe_2$ to $Nb_{1.05}Se_2$, T_c goes from 7.0°K to about 2.2°K in a regular manner. They report superconducting transition widths (ΔT) of the order of 1-2°K for samples between the composition of $Nb_{1.03}Se_2$ to $Nb_{1.05}Se_2$. Antonova et al.[7] studied three ranges of composition: 31.7-33.3 atomic percent (at. %) niobium ($Nb_{.95}Se_2$ - $NbSe_2$), 33.3-33.7 at. % niobium ($NbSe_2$ - $Nb_{1.01}Se_2$) and 33.7-34.3 at. % niobium ($Nb_{1.01}Se_2$ - $Nb_{1.03}Se_2$). In the range of $Nb_{.95}Se_2$ to $NbSe_2$, this group observed that T_c dropped from 7.0°K to 6.8°K at $Nb_{.95}Se_2$. This drop was associated with the formation of vacancies in the niobium sublattice without any change in the selenium sublattice. These results, as well as those cited below, were obtained from x-ray line intensities from which atomic

scattering factors could be estimated. When the niobium content was increased above stoichiometry ($NbSe_2$) no changes in T_c were observed until a critical vacancy concentration corresponding to $Nb_{1.01}Se_2$ was reached.[7] At this concentration it was shown that niobium atoms were being displaced from the lattice sites and a depression of T_c occurred.

Transition temperatures were shown to decrease in a regular manner to a value near 2°K at a composition of $Nb_{1.03}Se_2$[7]. Transition widths (ΔT) were observed to increase from a value of 0.2°K at stoichiometry as the niobium concentration increased. Antonova et al.[7] associated an ordering of the displaced niobium atoms, which is retained over the range $Nb_{1.01}Se_2$ to $Nb_{1.03}Se_2$, with singularities on the superconducting transition curves and the regular behavior of these singularities with increasing niobium concentration. Thus, it was the interpretation of Antonova et al.[7] that the rearrangement of the niobium sublattice has a significant influence on the superconductivity of 2H-$NbSe_2$.

Estimates from concentration versus T_c data presented by Revolinsky et al.[2] indicate those DVT crystals grouping around the transition temperature of 6.6°K have a composition of $Nb_{1.005}Se_2$ while the same type of estimate from the data of Antonova et al.[7] yields a concentration of $Nb_{1.01}Se_2$. The compositional values are consistent with the ΔT values observed for all DVT samples which were <0.2°K. The difference in the estimates from these works is related to the inabilities of these workers to produce consistent reproducible compositions[2]. Although DVT 4A (T_c=6.61°K) and DVT 6A (T_c=6.56°K) were grown in selenium rich atmospheres they also appear to be niobium rich. The XPS data for DVT 4A indicated excess niobium or a low oxidation state of niobium was

present on both the "as grown" and cleaved surfaces. The T_c's observed for these samples are below the value of 6.8°K observed by Antonova et al.[7] for the composition of 31.7 at. % niobium ($Nb_{.95}Se_2$).

3. The Effect of Iodine on Low Temperature Transport Properties

An examination of the T_c data for the DVT's and IVT's studied shows the T_c values for the IVT's to be consistently higher than the values observed for the DVT samples (Table IV). The average of the four highest DVT transition temperature values is 7.07 ± 0.02°K while the average for all four IVT crystals studied in this work is 7.20 ± 0.02°K. When reviewing the supporting data that was collected for these samples, the following observations must be considered.

It has been shown that the XPS spectra for the "as grown" surfaces of the DVT's are chemically unlike those of the IVT's, but the cleaved surfaces of each, which should be typical of the bulk, are very similar. Since the superconducting properties of these materials are determined more by the bulk than the surface properties, these surface differences do not appear to be significant. Since the same XPS spectra were observed for the oxidation state of niobium in cleaved DVT and IVT samples having T_c values over the range of 6.5 to 7.2°K, there does not appear to be a correlation with T_c and the XPS spectra for this energy region. XPS spectra were obtained for DVT and IVT crystals in the 0 to 25 eV region but the resolution was not high enough to resolve differences in the electronic density of states near the Fermi level.

One difference that exists between these samples is the quantity of iodine contained in the bulk. The XPS spectrum of IVT 1C powder showed iodine to be present as iodide ion. Neutron activation analysis

indicated the level of iodine in the IVT's is between 400 and 700 ppm while no detectable quantity, i.e., >5 ppm could be found in the DVT's (Table V). Other impurities were found but one of the most consistent differences appears to be in the iodine content. To confirm that some of the iodine was contained in bulk, a sample from IVT 1A was ground, washed in carbon tetrachloride, and allowed to stand in carbon tetrachloride for three weeks. A repeat analysis of the ground portion indicated 400 ppm iodine was present while 310 ppm was found in the washed portion. (The error in these measurements is about ± 10%.) Thus, it would appear that a major portion of the iodine detected for these samples is contained in the bulk. This level is comparable to the value of 100 ppm published by Myers and Monet[23] for IVT crystals. In the work of Huntley and Frindt[11], up to 1.5% iodine was found in IVT crystals by x-ray fluorescence spectroscopy. Finally, it seems quite possible that single crystals grown at 1050°K in a container having a volume of approximately 35 cm^3 and containing a 16 gram charge of polycrystalline $NbSe_2$ along with the recommended concentration of iodine, 5 mg per cm^3 of container volume[21], could become contaminated with 400-700 ppm of iodine.

Since the DVT's were grown without iodine, and no detectable quantity of iodine could be found by neutron activation analysis in DVT crystals, it seemed reasonable to assume that the effect of iodine on the low temperature transport properties of 2H-$NbSe_2$ could be determined by diffusing iodine into DVT samples. When interpreting the results from these studies, it must be realized that diffusing iodine into a crystal after growth has occurred may not represent the same

TABLE V. NEUTRON ACTIVATION ANALYSIS OF DVT AND IVT CRYSTALS

CONTAMINANTS	SENSITIVITIES (μgm)	DVT 1[a]	DVT 2[a]	DVT 3[b]	DVT 5[b]	DVT 6[b]	IVT 1A[c]	IVT 1C[c]	Nb	Se
Co	0.14	9	7	17	20	21	4	14	14	
Cr	0.34			40	104	306			440	54
Cu	0.11	19	8	61	57	64	37			116
Fe	45.0	1052	1810	3375	4900		1110	4700	1920	
I	0.0026						400	670		
K	0.057	76		93	116	119	55			
Mn	0.002			58	74	129	22	14		
Na	0.0016	272	39	184	242	191	185	186		
Ta	0.088	28	13	95	79	61	4	13	262	
W	0.0016	49	24	42	35	29	200	68		56
Zn	0.046	34	13	1042	730	818	50	56	26	
Total (ppm)		1564	1929	5007	6357	1707	2107	5621	2648	216
RRR		133	133	21	21	19	39	41		

[a] The results for DVT 1 and DVT 2 are based on single crystals.

[b] The results for DVT 3, DVT 5 and DVT 6 are based on polycrystalline samples.

[c] The results for IVT 1A and IVT 1C are based on pieces cleaved from these crystals.

situation that exists when IVT crystals are grown and the iodine is incorporated in the lattice as the crystal grows.

DVT crystals from growths 1 and 2, which had high RRR values, were selected for these experiments on the basis that they represented a lattice of more defect free structure. DVT 1C and approximately 250 mg of DVT 1 polycrystalline powder were exposed to an iodine atmosphere for 120 hours at 1025°K. Afterwards neutron activation analysis of the DVT 1 powder indicated 29 ppm iodine. A carbon tetrachloride washed sample was not analyzed, but on the basis of other experiments a reduction in the level of iodine occurred as a result of washing with carbon tetrachloride. Following the heat treatment T_c decreased from 7.11 to 6.03°K and the RRR value dropped from 133 to 9 (Table VI).

Since significant changes in T_c and RRR were observed and only a small amount of iodine could be found, a second experiment was conducted with crystals DVT 2A and DVT 1D. Each crystal was divided into two pieces; half of each for heat treatment in vacuum and half of each to be heat treated with DVT 1 powder in an iodine atmosphere. The tubes containing these samples were placed in the furnace with the ends containing the samples touching to minimize the possibility of a temperature difference. These samples were held at 975°K for 100 hours. The results of this experiment have been presented in Table VI and Figure 20.

It appears from these experiments that heat treatment introduced lattice disorders since the RRR value decreased significantly for all samples undergoing heat treatment in vacuum and heat treatment in iodine atmosphere. In the case of the DVT 1D sample that was heat

TABLE VI. EFFECT OF HEAT TREATMENT AND IODINE DOPING ON THE TRANSITION TEMPERATURE (T_c) AND RESIDUAL RESISTANCE RATIO (RRR) OF DVT CRYSTALS

	DVT 1C	DVT 1D	DVT 2A
		"As Grown"	
T_c (°K)	7.12		7.08
ΔT (°K)	.17		.12
RRR	137		140
t(cm)	3.4×10^{-4}	2.2×10^{-4}	1.3×10^{-3}
		Heat Treatment In Vacuum[a]	
TEMP (°K)		975	975
TIME (HRS.)		100	100
T_c (°K)		<4.5[b]	7.09
ΔT (°K)			.10
RRR		4[c]	12
		Heat Treatment In Iodine Atmosphere[d]	
TEMP (°K)	1025	975	975
TIME (HRS.)	120	100	100
T_c (°K)	6.03	7.23	7.16
ΔT (°K)	.65	.08	.25
RRR	9	21	28
Iodine (ppm)[e]	29	167	167
		(111)	(111)

[a] DVT 1D and DVT 2A crystals were heat treated in the same tube.

[b] Sample was not superconducting at 4.5°K.

[c] RRR (300°K/4.5°K).

[d] DVT 1D and DVT 2A crystals were heat treated in the same iodine atmosphere.

[e] Iodine concentration was determined by neutron activation analysis of DVT 1 powder that was in tube with crystals. Values in parenthesis are for DVT1 powder that was washed with carbon tetrachloride.

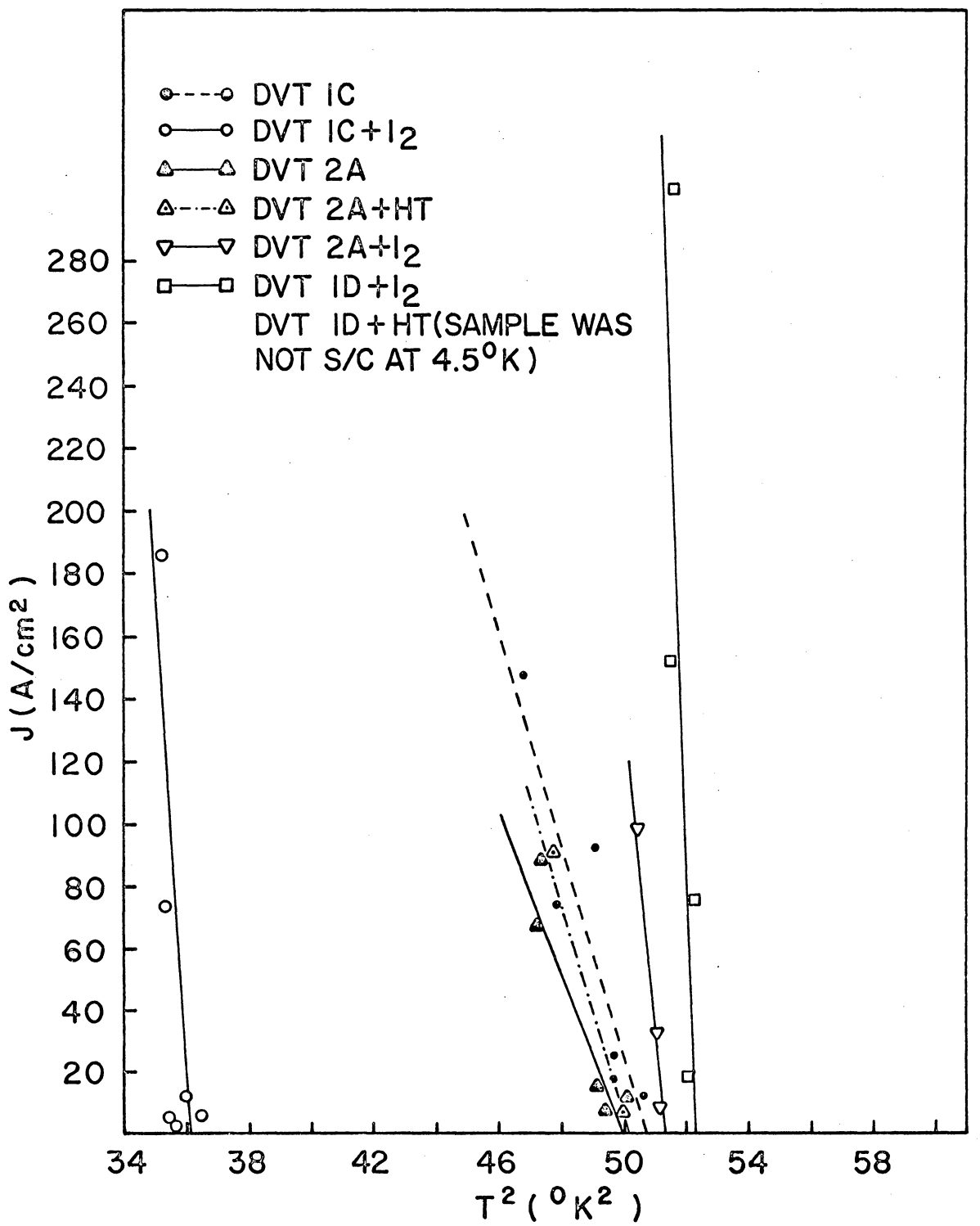

FIGURE 20. Effect of Heat Treatment in Vacuum and in Iodine Atmosphere on the Transition Temperature of 2H-$NbSe_2$ (DVT).

treated in vacuum, T_c was depressed to a temperature below 4.5°K. The reason for this depression is believed to be related to evaporation of selenium from the lattice. In the work by Antonova et al.[7] it was reported that in order to produce samples on the low selenium concentration side, a product of stoichiometric composition was annealed in a furnace with a steep temperature gradient so that selenium could be evaporated from the $NbSe_2$ lattice. A temperature gradient of 50°K over a length of 10 cm existed while DVT 1D was being heat treated. However, a limited amount of selenium would evaporate from the lattice to develop an equilibrium pressure in the tube if a temperature gradient did not exist. Since the iodine level that existed while DVT 1C was being heat treated was low, it is possible that the prevailing mechanism during this experiment was one of selenium evaporation from the lattice rather than iodine diffusion into the lattice. If this were the case, the decrease in T_c for DVT 1C would be explained by an increase of niobium content beyond the critical composition of $Nb_{1.01}Se_2$.

The interpretation of the results from the heat treatment of DVT 2A appear to be more difficult. It is apparent from the drop in RRR from 140 to 12 that disorder was introduced in the lattice yet T_c remained unchanged. Evaporation of selenium from the lattice should have occurred for this sample just as it occurred with the others. Since T_c did not decrease, it must be concluded that the critical composition of $Nb_{1.01}Se_2$ was not approached throughout the sample. The thickness of DVT 2A is about six times that of DVT 1D. Since the rate of selenium evaporation is somewhat controlled by the diffusivity of selenium atoms to the crystal surface, a thicker crystal would undergo a smaller com-

position change throughout per unit time than a thinner one. Thus, if the composition of the interior of the crystal was not changed sufficiently to depress T_c, then this region could short out the resistivity of the region closer to the surface. Since RRR is a property of the normal state, the disorder that is introduced into the surface or interior of the crystal will affect this property.

Neutron activation analysis of the DVT 1 powder that was heat treated with DVT 1D and DVT 2A indicated a higher concentration of iodine was present than that during the experiment with DVT 1C. These results show that after a three week soak in carbon tetrachloride 111 ppm iodine remained in the powder (Table VI). The T_c values observed for these crystals are higher than any observed for a DVT and are typical of those observed for the IVT's studied in this work. The RRR values fall within the range of 10 to 65 reported[35,36] in the literature for IVT samples. Thus, it appears that T_c has been enhanced by the presence of iodine.

Before attempting to explain the difference observed in T_c for IVT's and DVT's and also the changes in T_c resulting from iodine doping of DVT's, it will be necessary to discuss the parameters that affect T_c. It is known from the theory of Bardeen, Cooper, and Schieffer[37] that the superconducting transition temperature is given by an expression of the form:

$$T_c = 1.14\langle\omega\rangle \exp[-1/N(0)V] \qquad (6)$$

where $\langle\omega\rangle$ is a typical phonon energy, N(0) is the electronic density of states at the Fermi surface at zero temperature and V is the pairing

potential arising from the electron-phonon interaction. McMillan[38] has derived an expression for T_c based on the so-called "strong coupled" theory which has the following form:

$$T_c = \frac{\Theta}{1.45} \exp\left[-\frac{1.04(1+\lambda)}{\lambda-\mu^*(1+0.62\lambda)}\right] \tag{7}$$

In this expression the Debye Θ is used for the characteristic phonon frequency, μ^* is a Coulomb pseudopotential and λ is the electron-phonon coupling constant which is given by an expression of the form:

$$\lambda = \frac{N(0)\langle I^2\rangle}{M\langle\omega^2\rangle} . \tag{8}$$

In this expression N(0) is the density of states at the Fermi surface at zero temperature, $\langle I^2\rangle$ the average over the Fermi surface of the square of the electronic matrix element, $\langle\omega^2\rangle$ the average phonon frequency and M the atomic mass. Thus, from these equations it can be seen that the superconducting transition temperature is dependent upon the density of states at the Fermi surface, the phonon spectrum and the electron-phonon interaction.

It has been pointed out by Tsang et al.[25] that any attempt to interpret changes in T_c as a result of disordering of layered dichalcogenides must consider these three parameters. Tsang et al.[25] indicate that in many cases the changes in T_c for the layered dichalcogenides that have resulted from intercalation or the introduction of lattice disorder by other means have erronously been interpreted as a simple change in the density of states near the Fermi surface.

Figure 21 shows the conduction band structure for $NbSe_2$ as proposed by McMenamin and Spicer[39]. This figure, which is based on ultra-

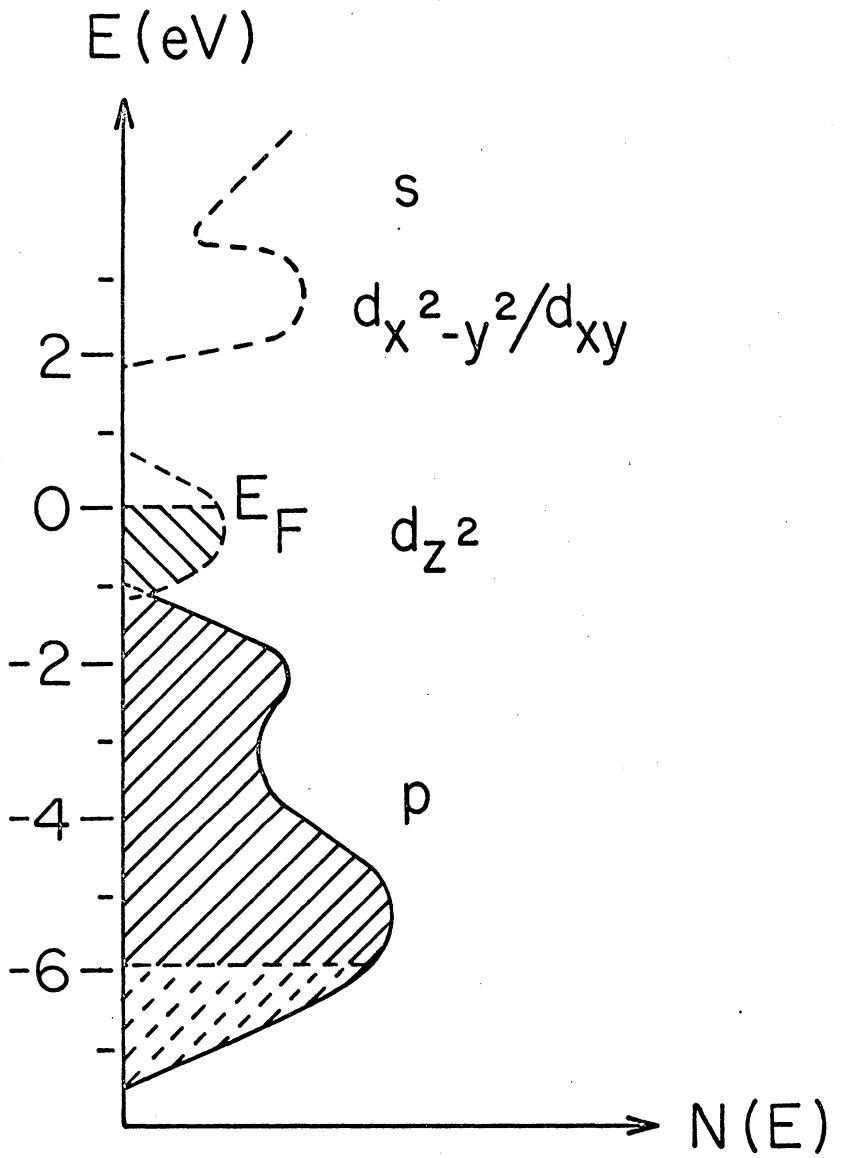

FIGURE 21. Electronic Band Structure for $NbSe_2$ (After McMenamin and Spicer[39]).

violet photoelectron studies, shows the d_z2 band to be partially empty with the Fermi level near a maximum in the electronic density of states N(E) where N(E) is the density of states at temperatures above absolute zero. One interpretation that has been used to explain changes in T_c of $NbSe_2$ when it is intercalated with sodium, potassium or organic molecules is that the atoms or molecules as the case may be donate a fraction of an electron to the d_z2 band and move the Fermi level up a small amount[39]. Since the slope of N(E) is negative at E_F it decreases, and therefore through the dependence of T_c upon N(E), T_c decreases.

Earlier it was shown that the XPS spectrum of IVT 1C powder indicated that iodine existed as iodide ion I^-. Therefore it is possible that electrons were removed from the d_z2 band by the iodine and thus N(E) increased. Since removal of electrons from the narrow d_z2 band by iodine would bring a change of N(E) in the right direction and N(E) is high at the Fermi level, it is possible that a very small contribution to the difference in the T_c values observed for IVT samples versus DVT samples is related to this mechanism. If the iodine concentration were greater than 400-700 ppm, then this mechanism could possibly account for more of the change. This tends to place more emphasis on the dependence of T_c upon changes in the phonon spectrum and the electron-phonon interaction at the Fermi surface.

Perhaps the most straightforward manner to demonstrate the effect of iodine upon the electron-phonon interaction is to consider the following sequence of experiments published by others.

(a) Huntley and Frindt[11] were able to eliminate the sign reversal in the Hall coefficient that normally occurs for $NbSe_2$ around 26°K with

about one percent iodine impurity.

(b) The change in sign of the Hall coefficient of $NbSe_2$ is related to a low temperature crystallographic structure change[13,40].

(c) Tsang et al.[25] have demonstrated that electronic band structure is sensitive to small changes in crystal structure and therefore it is incorrect to assume that the electron-phonon interaction parameter is independent of crystallographic changes.

This sequence of experiments indicate that small quantities of iodine can significantly affect the crystallochemical properties of $NbSe_2$. The exact manner in which iodine brings about these changes has not been resolved.

4. Tunneling Measurements

Tunneling measurements were included in this work to get a better understanding of how iodine affects the electron-phonon interaction parameter and also to extend the characterization of the DVT samples to another area. Although these experiments were not as successful as hoped, the results will be discussed because of their significance to future work. A brief description of the application of electron tunneling measurements to study the superconducting state of a material is given below.

The superconducting energy gap is predicted by the theory of Bardeen, Cooper, and Schriefer and has been confirmed experimentally by specific heat, nuclear relaxation, electromagnetic absorption, and electron tunneling measurements[41]. From electron tunneling measurements the superconducting energy gap, the density of states at the Fermi surface N(E), and in some cases information concerning the phonon

spectrum of the material can be determined.

The mechanism of electron tunneling is not peculiar to superconductors. Electron tunneling can occur between two metals in the normal state separated by a thin insulating film. The ability of electrons to penetrate a potential barrier is predicted quantum mechanically. The thickness of the potential barrier is critical to electron tunneling since the transmission coefficient depends exponentially upon the barrier thickness and upon the square root of the height of the barrier. When both metals are normal the current versus voltage relationship for the junction is ohmic. This stems from the linear dependence of the tunneling current upon the electron density of states in the metals on either side of the barrier. A diagram of the density of states for the metals and the current versus voltage relationship for a normal metal-insulator-normal metal junction is given in Figure 22.

When one of the metals in the junction becomes a superconductor the current versus voltage relationship becomes nonlinear at low voltages. At zero temperature no current can flow until the applied voltage is equal to one half the energy gap. Applying a potential of this value enables electrons to tunnel across the barrier in a direction determined by the polarity of the applied voltage. As the voltage is increased beyond the gap value, the current versus voltage characteristics approach that of two metals in the normal state (Figure 22).

The normalized tunnel conductance is obtained for a metal-insulator-superconductor junction from derivative measurements on the tunneling current versus voltage curve. Normalized conductance is defined as

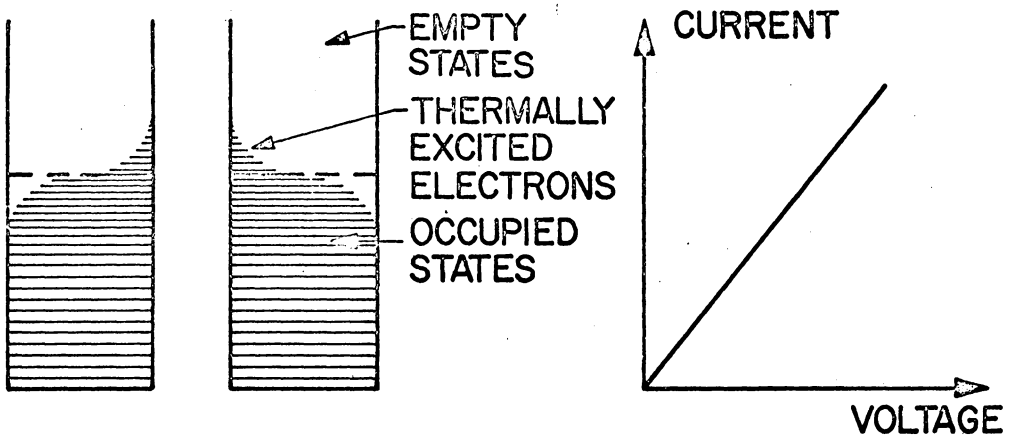

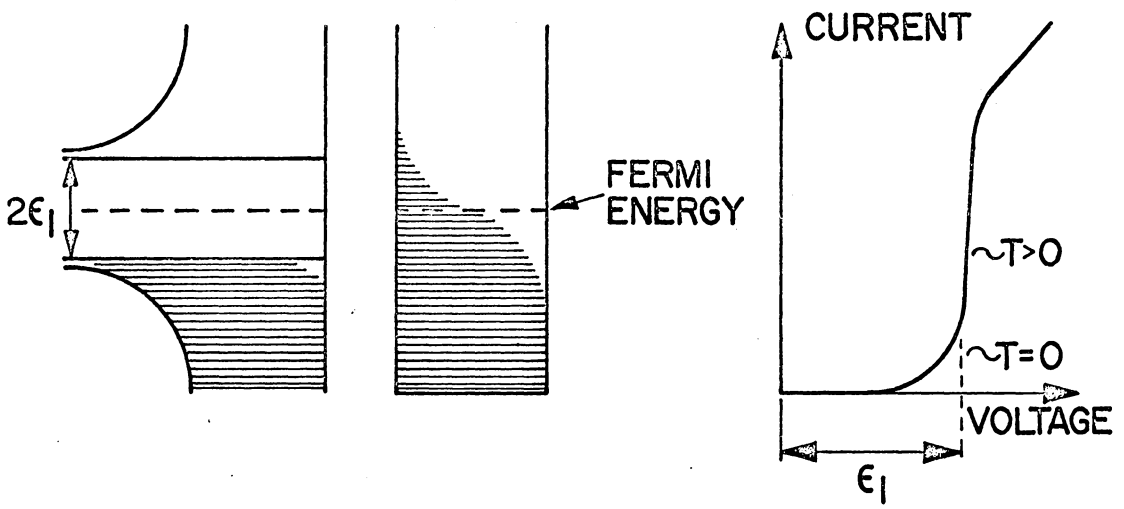

FIGURE 22. Energy Diagrams and Current-Voltage Characteristics For Tunnel Junctions. (a) Two Metals in the Normal State Separated by a Barrier; (b) A Metal in the Normal State and a Metal in the Superconducting State Separated by a Barrier. (After Giaever and Megerle[41]).

$$\sigma(v) \equiv \frac{dI_{NS}/dV}{dI_{NN}/dV} = \frac{|eV|}{[(eV)^2-\Delta^2]^{1/2}} = \frac{N(E)_s}{N(0)} \qquad (9)$$

where dI_{NS}/dV is the conductance of the junction in the superconducting state, dI_{NN}/dV is the conductance of the junction in the normal state, $N(E)_s$ is the density of states in the superconductor; N(0) the density of states in the normal metal, 2Δ the magnitude of the energy gap and V the applied voltage[42]. Thus the density of state in the superconductor can be written

$$N(E)_s = \frac{N(0)[E]}{(E^2-\Delta^2)^{1/2}} . \qquad (10)$$

Figure 23 is a conductance vs voltage curve for a Pb-MgO-Mg junction observed by Giaever et al.[43] at 0.33°K. This curve shows a sharp increase in $\sigma(V)$ near the gap edge, as predicted by the expression (9) above, and a decrease in $\sigma(V)$ as the voltage is raised above the gap value. The deviations in the curves at 4ε and 8ε, which are not predicted by the conductance expression given above, have been induced through the electron-phonon interaction. These energies correspond to peaks in the lead phonon spectrum.

Several tunnel junctions were fabricated for DVT and IVT samples using carbon as a barrier. Carbon was chosen as a barrier material because it has successfully been used on metal surfaces that do not oxidize uniformly and it is metallurgically inert[44,45,46]. When the tunneling effort was initiated, junctions were formed with tin counter-electrodes. Several $NbSe_2$/C/Sn junctions were fabricated that had a resistance of less than one ohm. When defects exist in the junction as a result of imcomplete coverage of the superconductor surface, or if the

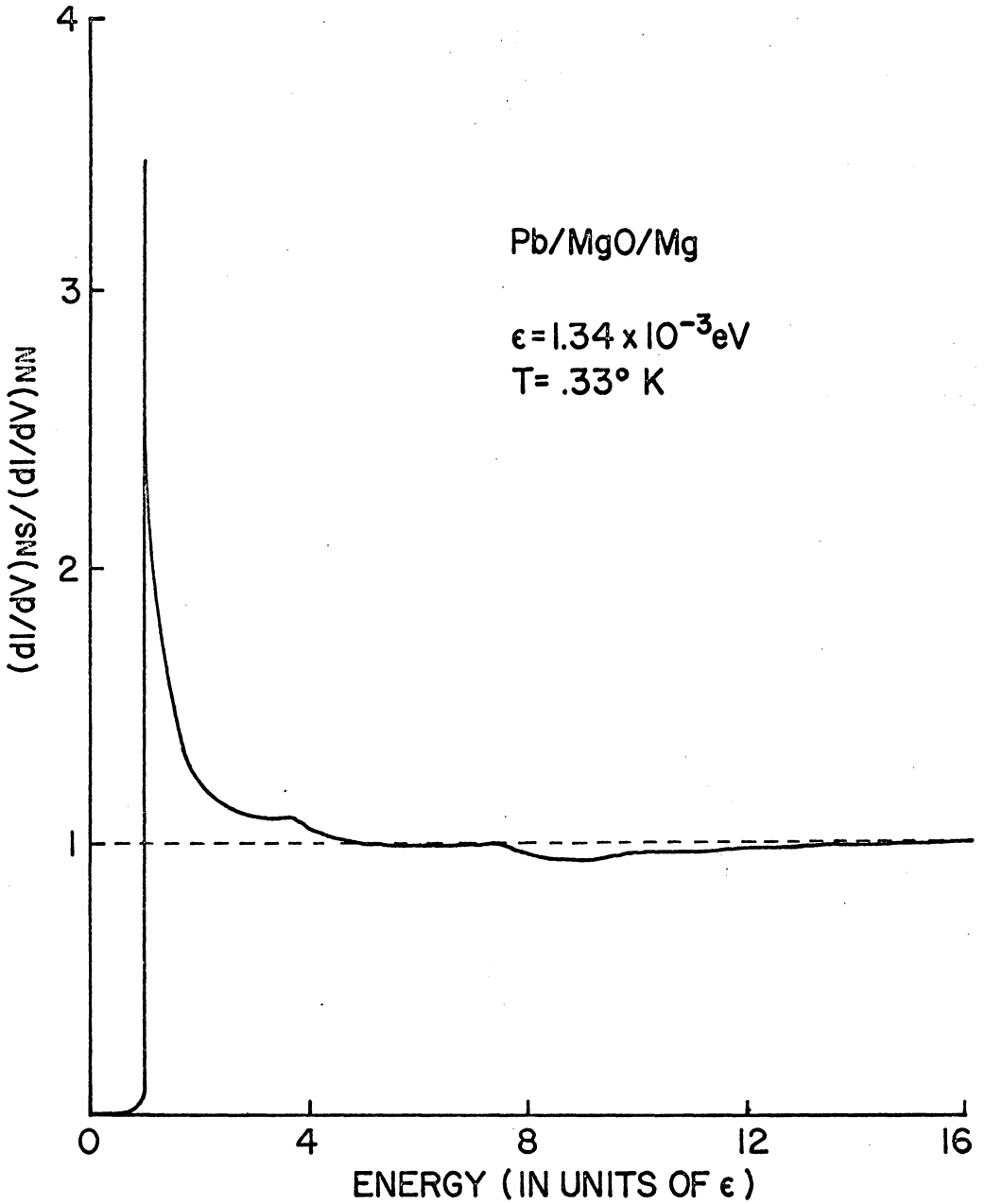

FIGURE 23. The Relative Conductance of Pb-MgO-Mg Sandwich as a Function of Energy (After Giaever et al.[43]).

barrier is electrically or physically damaged, non-tunneling currents will flow and the gap voltage cannot be resolved with accuracy. The problem of low resistance across the $NbSe_2$/C/Sn junctions was thought to be caused by the contacts on the multiprobe sample holder mechanically rupturing the thin carbon and tin layers. Several attempts to form thicker electrodes were made before a junction with a resistance of greater than 100 ohms was obtained. The junctions with thick tin electrodes were difficult to form because of a tin dewetting and adhesion problem.

To circumvent the problem of tin dewetting, several junctions were formed with lead counterelectrodes. Even though thicker electrodes readily could be formed the problem with low junction resistance remained. Junctions were fabricated on gold substrates to determine if the low junction resistance was related to the $NbSe_2$ surface conditions. Numerous Pb/C/Au junctions were fabricated before one was made having a resistance high enough to observe the lead energy gap. Several experiments that involved substrate preparations, metal electrode and carbon evaporation cycles, and variation of junction crossectional areas were conducted to correct the problem of low resistance without success. After the completion of these studies, it was concluded that the problem of low junction resistance was related to defects in the carbon barriers and not the mechanical movements of the electrical contacts.

The tunneling measurements taken from one of the better $NbSe_2$/C/Sn junctions is presented in Figure 24. The temperature dependence of the energy gap is given a good approximation[37] by the following expression

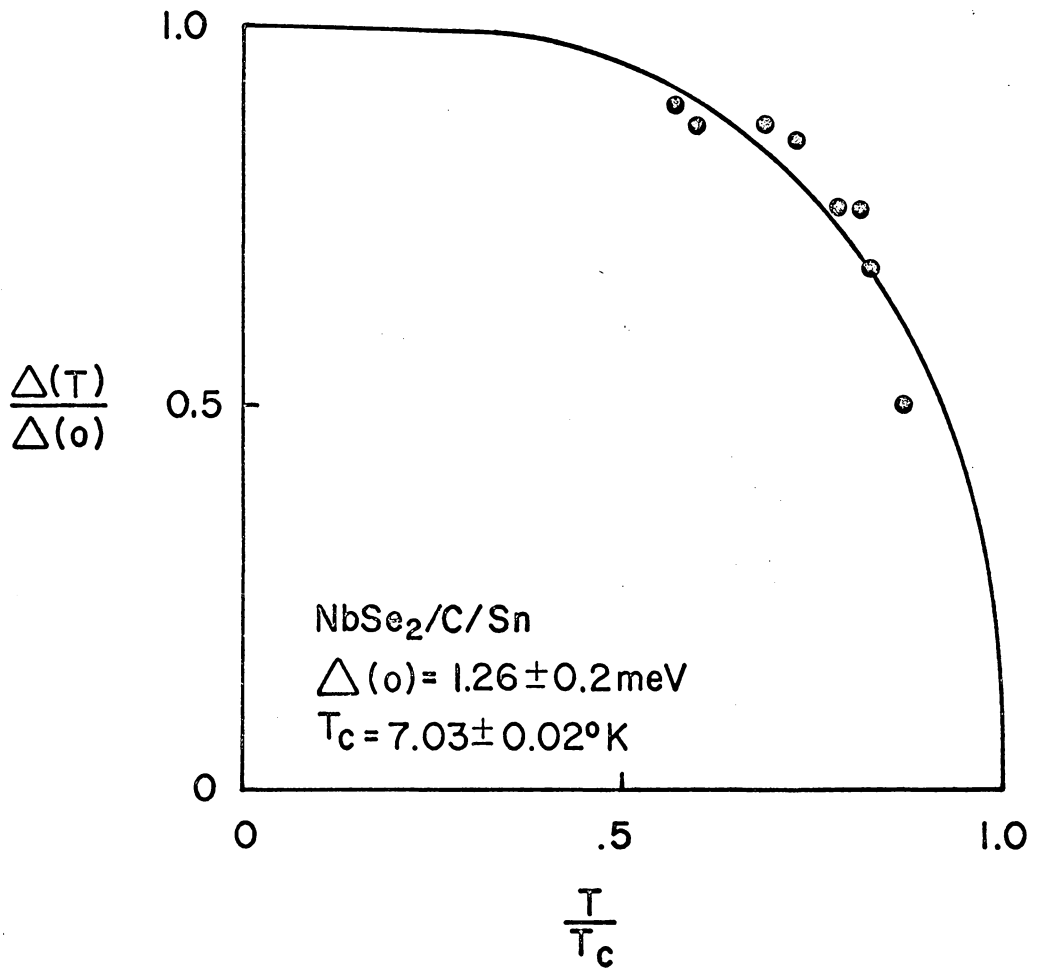

FIGURE 24. The Reduced Energy Gap as a Function of Temperature for a DVT 2 Sample (—— BCS Theory).

$$\frac{\Delta(T)}{\Delta(0)} = \tanh\left[\left(\frac{T_c}{T}\right)\left(\frac{\Delta(T)}{\Delta(0)}\right)\right] \qquad (11)$$

where $2\Delta(T)$ is the energy gap at temperature T and $2\Delta(0)$ is the energy gap at zero temperature. From this curve the value of $\Delta(0)$ for this DVT 2 crystal was estimated to be 1.26 ± 0.2 meV. This value is higher than the value of 0.62 ± 0.04 meV for a $NbSe_2$/C/Pb junction reported by Morris and Coleman[36]. The energy gap in 2H-$NbSe_2$ is known to be anisotropic from infrared measurements. The value of the energy gap for electrons flowing parallel to the layers was reported to be 1.13 meV[17]. Tunneling measurements give the value of the energy gap perpendicular to the layers. Two possible explanations are offered for the observed value of 1.26 ± 0.2 meV obtained by tunneling. One possibility is that the energy gap of the DVT 2 sample is significantly higher than the IVT samples that have previously been studied. The other possibility is that crystal misorientation may have existed in the junction area and the energy gap parallel to the layers rather than that perpendicular to the layers was observed.

As a result of the high conductance observed for all of the junctions made with carbon barriers and the many anomalous effects observed in the derivatives of the current-voltage curves, attempts to study DVT junctions as a function of iodine doping were abandoned. A more reproducible means of fabricating the junction is essential.

IV. CONCLUSIONS

A. Summary

A procedure for the growth of single crystals of 2H-$NbSe_2$ by a direct vapor transport (DVT) mechanism was developed. This procedure permits high purity single crystals of this material to be grown. Residual resistance ratio values of 130 to 140 have been obtained which are significantly higher than the values of 10 to 65 that have been reported in the literature for samples prepared by the iodine vapor transport (IVT) procedure. It was demonstrated that the chemical composition of the starting material has a significant effect upon growth conditions which in turn affects the superconducting transition temperature and residual resistance ratio. It was concluded that selenium acts as a transporting agent for the growth of the single crystals.

X-ray diffraction measurements were used to show that crystals grown by direct vapor transport and iodine vapor transport procedures have the same structure. A correlation was not found between crystal defects, as viewed from transmission Laue patterns, and residual resistance ratios.

X-ray photoelectron measurements were made of the oxidation state of niobium on the surface and in the bulk of 2H-$NbSe_2$. These measurements indicated the niobium on the surfaces of the IVT samples was more completely oxidized than the niobium on the surface of the DVT samples. X-ray photoelectron measurements indicated cleaved DVT and IVT surfaces are similar. In both cases more niobium, which was identified as Nb°, appeared to be present on the cleaved surfaces than is consistent with

the chemical formula $NbSe_2$ and the superconducting transition temperatures observed for these samples.

X-ray photoelectron spectroscopy studies were used to show that the valence state of iodine incorporated in the lattice of the IVT samples is consistent with the iodine existing as iodide ion. The presence of iodine in the IVT samples was confirmed by neutron activation analysis.

A critical current density dependence upon crystal thickness was observed for the DVT and IVT samples. The higher critical current densities that were observed for the DVT crystals were attributed primarily to thickness. The possibility that the DVT samples may possess higher upper critical fields (Hc_2) was not discounted.

The superconducting transition temperatures of the DVT crystals with high RRR values were observed to be about 0.1°K lower than those observed for the IVT crystals. It was demonstrated by means of iodine doping of the DVT crystals that the superconducting transition temperature of 2H-$NbSe_2$ was elevated by iodine. The difference in the superconducting transition temperatures observed for the DVT and IVT samples was attributed to the presence of iodine. The mechanism by which iodine elevates the transition temperature of 2H-$NbSe_2$ is not clear. It is believed that the mechanism is more dependent upon the electron-phonon interaction than a simple electron filling of the d band.

In conclusion the availability of single crystals of 2H-$NbSe_2$ free of a halide transporting agent has allowed data regarding the superconducting state of this compound to be studied that until the present time was not possible.

B. Recommendations For Future Work

A natural extension of this work would involve the preparation of 2H-$NbSe_2$ single crystals by the DVT procedure using higher purity niobium than that used in this work, i.e., greater than 99.8% pure and longer initial reaction times. The purpose of this type of study would be to determine if RRR values above those reported in this work could be attained.

Additional x-ray photoelectron spectroscopy measurements on cleaved 2H-$NbSe_2$ surfaces and compounds containing niobium in the Nb^{2+} oxidation state would be informative. This work could provide additional information regarding the crystallochemical nature of 2H-$NbSe_2$.

In view of the current interest in the relationship that exists between charge density waves, low temperature lattice distortions, and the change in sign of the Hall coefficient at about 26°K, it may be informative to see what effects are observed when DVT crystals of high RRR are subjected to this type of study.

Iodine doping studies at higher levels than those used in this work performed in conjunction with transition temperature and critical field measurements may provide additional information about the superconducting state of 2H-$NbSe_2$.

Tunneling measurements designed to study the effect of iodine on the electron-phonon interaction in $NbSe_2$ appear to be desirable. However, before these studies can be performed a consistent method for fabricating tunnel junctions will have to be developed. Junctions formed as Al/Al_2O_3/Al/$NbSe_2$ that function by the proximity effect may provide a more consistent means for performing tunneling measurements than junc-

tions based on carbon barriers.

V. REFERENCES

1. J. A. Wilson and A. D. Yoffe, Adv. Phys. 18, 193 (1969).

2. E. Revolinsky, B. E. Brown, D. J. Beerntsen and C. H. Armitage, J. Less Common Metals 8, 63 (1965).

3. A. H. Thompson, Phys. Rev. Lett. 34, 520 (1975).

4. W. A. Little, Phys. Rev. 134, A1416 (1964).

5. V. L. Ginzburg, Soviet Phys. JETP Engl. Transl. 47, 2318 (1964).

6. F. R. Gamble, F. J. Di Salvo, R. A. Klemm, and T. H. Geballe, Science 168, 568 (1970).

7. A. Antonova, K. V. Kiseleva, and S. A. Medvedev, Fiz. Metallov i Metallovedenie 27, 441, (1969).

8. G. A. Spiering, E. Revolinsky, and D. J. Beerntsen, J. Phys. Chem. Solids 27, 535 (1966).

9. E. A. Antonova, S. A. Medvedev, and I. Yu Shebalin, Zh. Eksp. Teor. Fiz. 57, 329 (1969) [Sov. Phys. - JETP 30, 181 (1970)].

10. H. N. S. Lee, H. McKinzie, D. S. Tannhauser, and A. Wold, J. Appl. Phys. 40, 602 (1969).

11. D. J. Huntley and R. F. Frindt, Can. J. Phys. 52, 861 (1974).

12. K. Yamaya and T. Sambongi, Solid State Comm. 11, 903 (1972).

13. M. Marezio, P. D. Dernier, A. Menth, and G. W. Hull, Jr., J. Solid State Chem. 4, 425 (1972).

14. J. A. Wilson, F. J. Di Salvo, and S. Mahajan, Phys. Rev. Lett. 32, 882 (1974).

15. J. Edwards and R. F. Frindt, J. Phys. Chem. Solids 32, 2217 (1971).

16. R. F. Frindt, R. B. Murray, G. D. Pitts, and A. D. Yoffe, J. Phys. C: Solid State Phys. 5, 154 (1972).

17. B. P. Clayman, Can. J. Phys. 50, 3193 (1972).

18. R. C. Morris and R. V. Coleman, Phys. Lett. 43A, 11 (1973).

19. D. H. Lee, L. W. Dubeck, and F. Rothwarf, Phys. Lett. 53A, 379 (1975).

20. H. Schafer, Z. Anorg. Allgem., 286 (1956).

21. R. Nitsche, H. U. Bolsterli and M. Lichtensteiger, J. Phys. Chem. Solids 21, 199 (1961).

22. R. Kershaw, M. Vlasse and A. Wold, Inorg. Chem. 8, 1599 (1967).

23. G. E. Myers and G. L. Montet, J. Phys. Chem. Solids 32, 2646 (1971).

24. N. E. Lewis, T. E. Leinhardt and J. G. Dillard, Mat. Res. Bull. 10, 967 (1975).

25. J. C. Tsang, M. W. Shafer, and B. L. Crowder, Phys. Rev. B 11, 155 (1975).

26. J. Kopp, D. J. Huntley, and R. F. Frindt, Con. J. Phys. 50, 2840 (1972).

27. R. D. Seals, R. Alexander, L. T. Taylor, and J. G. Dillard, Inorg. Chem. 12, 2485 (1973).

28. K. R. Milkove, B. S. Thesis; unpublished, M.I.T., Dept. of Physics (1975).

29. J. G. Adler and J. E. Jackson, Rev. Sci. Instru. 37, 1049 (1966).

30. G. E. McGuire, G. K. Scheweitzer, and T. A. Carlson, Inorg. Chem. 11, 2450 (1973).

31. F. Kadijk, R. Huisman, and F. Jellinek, Rec. Trav. Chim. 83, 768 (1964).

32. C. S. Fadley, S. B. M. Hagstrom, M. P. Klein, and D. A. Shirley, J. Chem. Phys. 48, 3779 (1968).

33. Y. B. Kim and M. J. Stephen, In Superconductivity 2, edited by R. D. Parks (Marcel Dekker, Inc., New York), 1107 (1969).

34. J. R. Long, N. E. Lewis, D. Agosta, and N. K. Batra, Bull. A.P.S. 21, 291 (1976).

35. B. P. Clayman and R. F. Frindt, Solid State Comm. 9, 1881 (1971).

36. R. C. Morris, R. V. Coleman, and R. Bhandari, Phys. Rev. B 5, 895 (1972).

37. J. Bardeen, L. N. Cooper, and Schrieffer, Phys. Rev. 106, 162 (1957); 108, 1175 (1957).

38. W. L. McMillan, Phys. Rev. 167, 331 (1968).

39. J. C. McMenamin and W. E. Spicer, Phys. Rev. Lett. 29, 1501 (1972).

40. J. A. Wilson, F. J. Di Salvo, and S. Mahajan, Adv. in Phys. 24, 117 (1975).

41. I. Giaever and K. Megerle, Phys. Rev. 122, 1101 (1961).

42. J. R. Schrieffer, "Tunneling Phenomena in Solids", (edited by E. Burstein and S. Lundquist), p. 287. Plenum Press, New York (1969).

43. I. Giaever, H. R. Hart, Jr., and K. Megerle, Phys. Rev. 126, 941 (1962).

44. M. L. A. MacVicar, S. M. Freake, and C. J. Adkins, J. Vac. Sc. and Tech. 6, 717 (1969).

45. M. L. A. MacVicar, J. Appl. Phys. 41, 4765 (1970).

46. S. I. Ochiai, M. L. A. MacVicar, and R. M. Rose, Phys. Rev. B 4, 2988 (1971).

The vita has been removed from the scanned document

SUPERCONDUCTIVITY AND LOW TEMPERATURE PROPERTIES OF NIOBIUM DISELENIDE SINGLE CRYSTALS GROWN BY DIRECT VAPOR TRANSPORT

by

Norris Earl Lewis

(ABSTRACT)

A procedure for the growth of high purity single crystals of 2H-$NbSe_2$ by a direct vapor transport (DVT) method was developed. Single crystal growth rate and the degree of crystal perfection were studied as deviations from stoichiometry were made over the compositional range of $Nb_{0.95}Se_2$ to $Nb_{1.05}Se_2$. Single crystal perfection was also studied as changes were made in the reaction and annealing times. Residual resistivity ratio (RRR) values were observed over the range of 21 to 140 and superconductivity was observed over the range of 6.60°K to 7.12°K as growth conditions were varied. It was concluded that selenium acts as a transporting agent for the growth of the single crystals.

X-ray photoelectron spectroscopy (XPS) measurements were made of the oxidation state of niobium on the surface and in the bulk of 2H-$NbSe_2$ samples prepared by the DVT and iodine vapor transport (IVT) procedures. These measurements indicated the niobium on the surface of the IVT samples was more completely oxidized than the niobium on the surface of the DVT samples, whereas, XPS spectra of cleaved DVT and IVT surfaces were similar. In both cases more niobium, which was identified as Nb°, appeared to be present on the cleaved surfaces than is consistent with the chemical formula $NbSe_2$ and the superconducting transition tempera-

tures observed for these samples. X-ray photoelectron spectroscopy measurements made of the $3d_{3/2}$ level of iodine incorporated in the lattice of the IVT samples indicated the iodine is present as iodide ion.

A critical current density dependence upon crystal thickness was observed for the DVT and IVT samples. The higher critical current densities that were observed for the DVT crystals were attributed primarily to thickness.

The superconducting transition temperatures of the DVT crystals with the highest degree of crystal perfection were observed to be about 0.1°K lower than those observed for the IVT crystals. It was demonstrated by means of iodine doping of the DVT crystals that the superconducting transition temperature of 2H-$NbSe_2$ was elevated by iodine.